

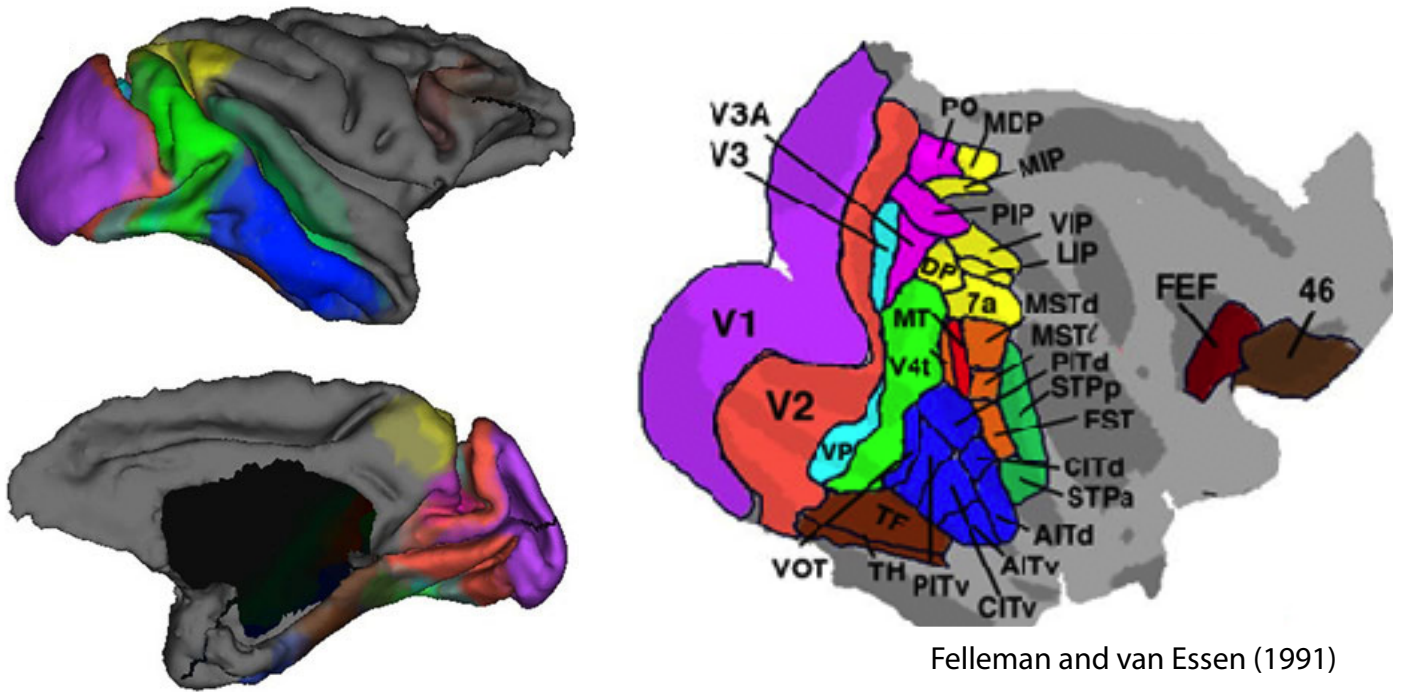
# Neural circuits for direction selectivity in visual cortex

**Wyeth Bair**

**Biological Structure  
University of Washington  
Seattle, WA**

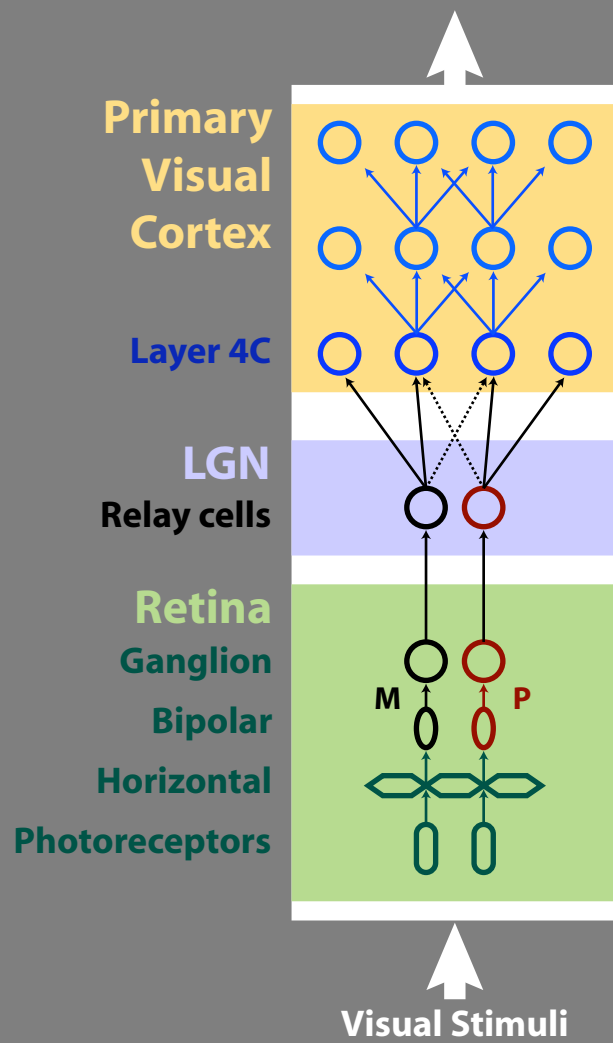
---

# Macaque visual cortex

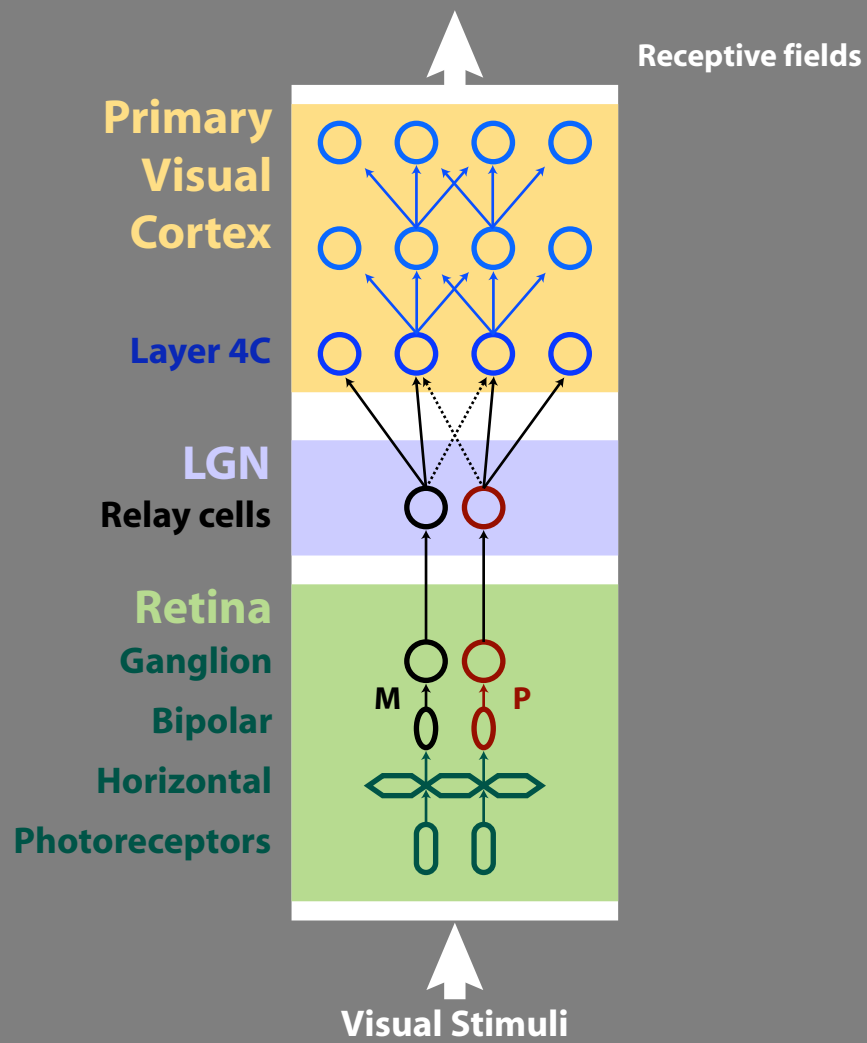


David C. van Essen, In: Visual Neurosciences, 2003 (L. Chalupa, J. Warner, eds.)

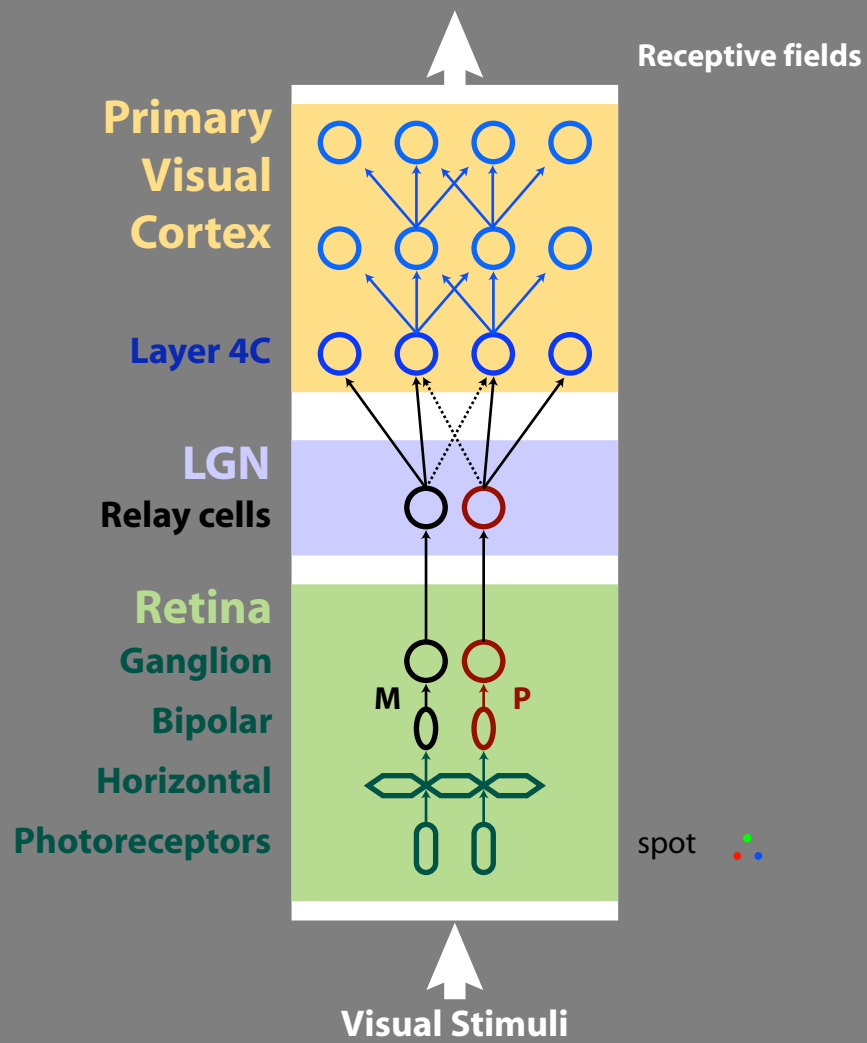
# The visual motion pathway from retina to V1



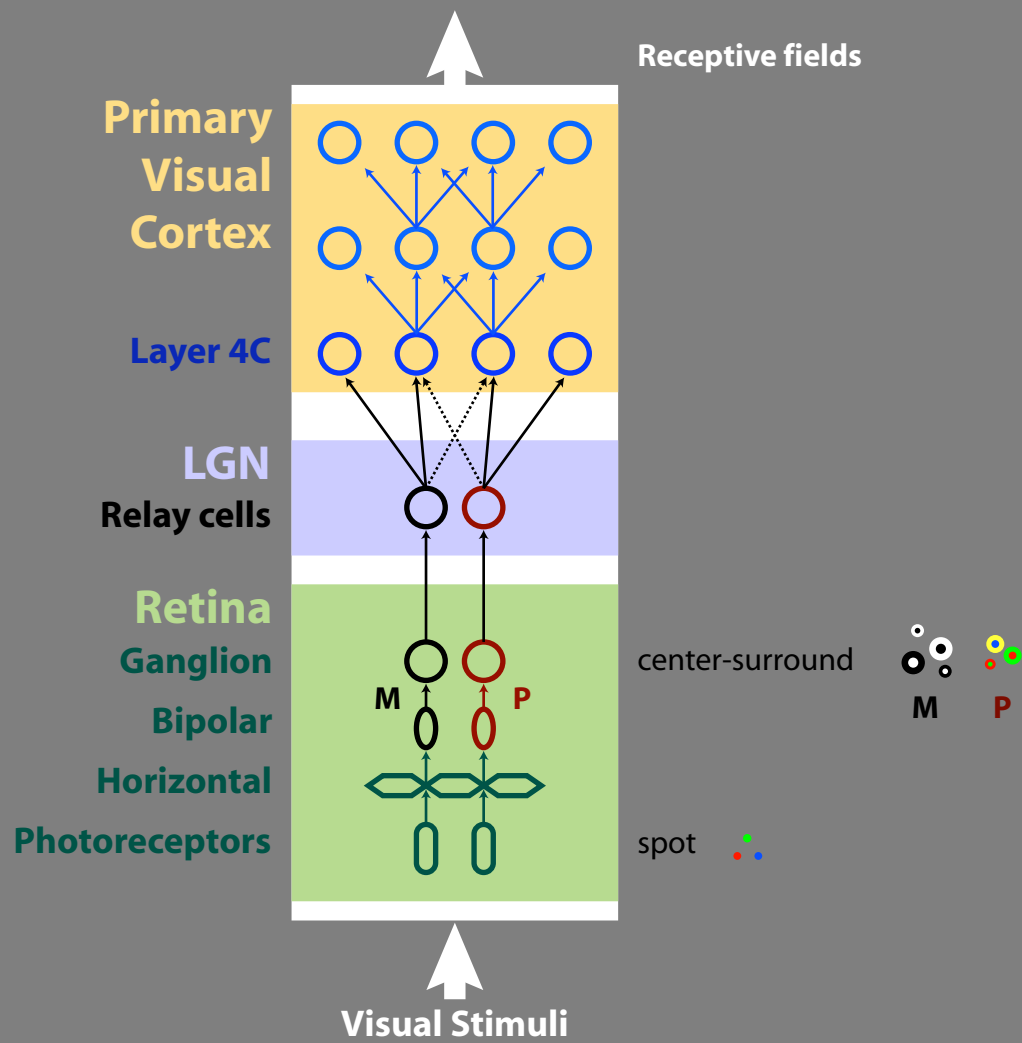
# The visual motion pathway from retina to V1



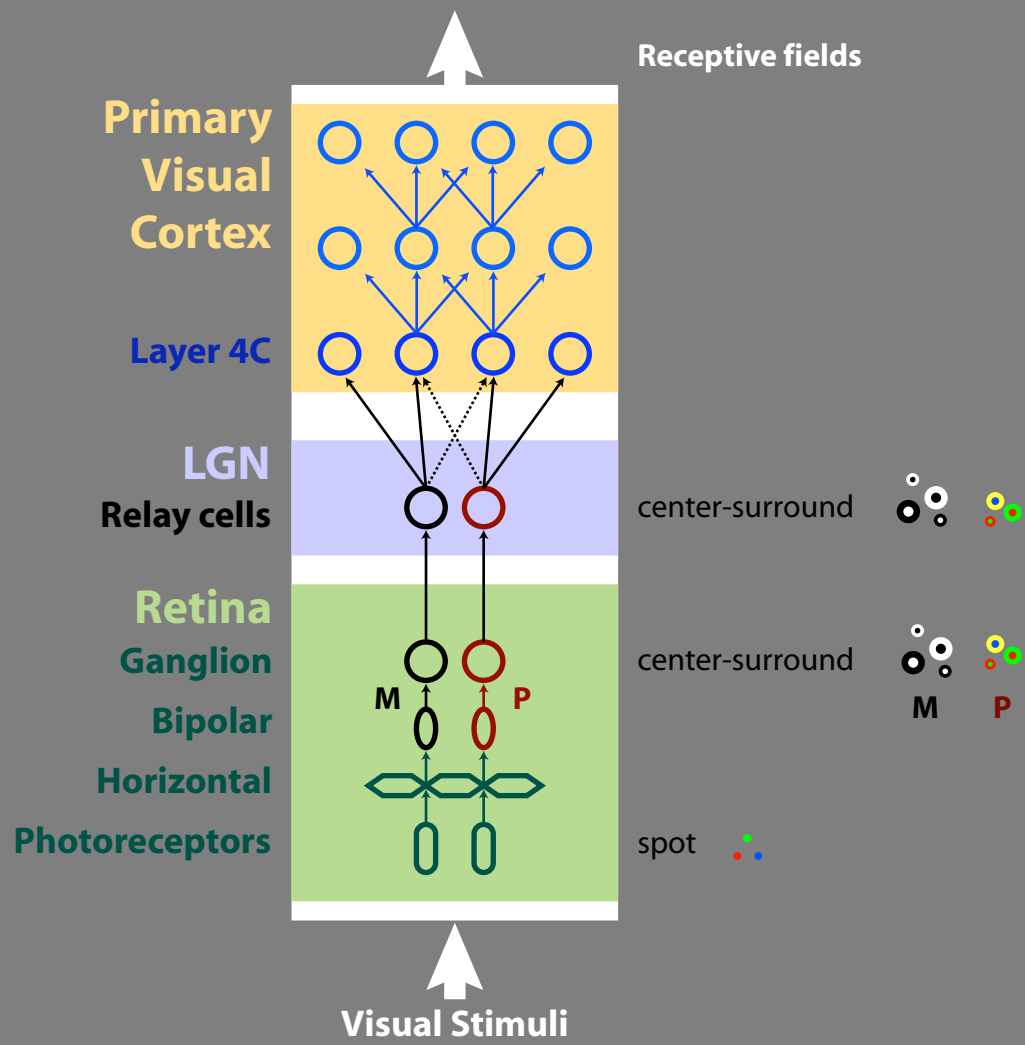
# The visual motion pathway from retina to V1



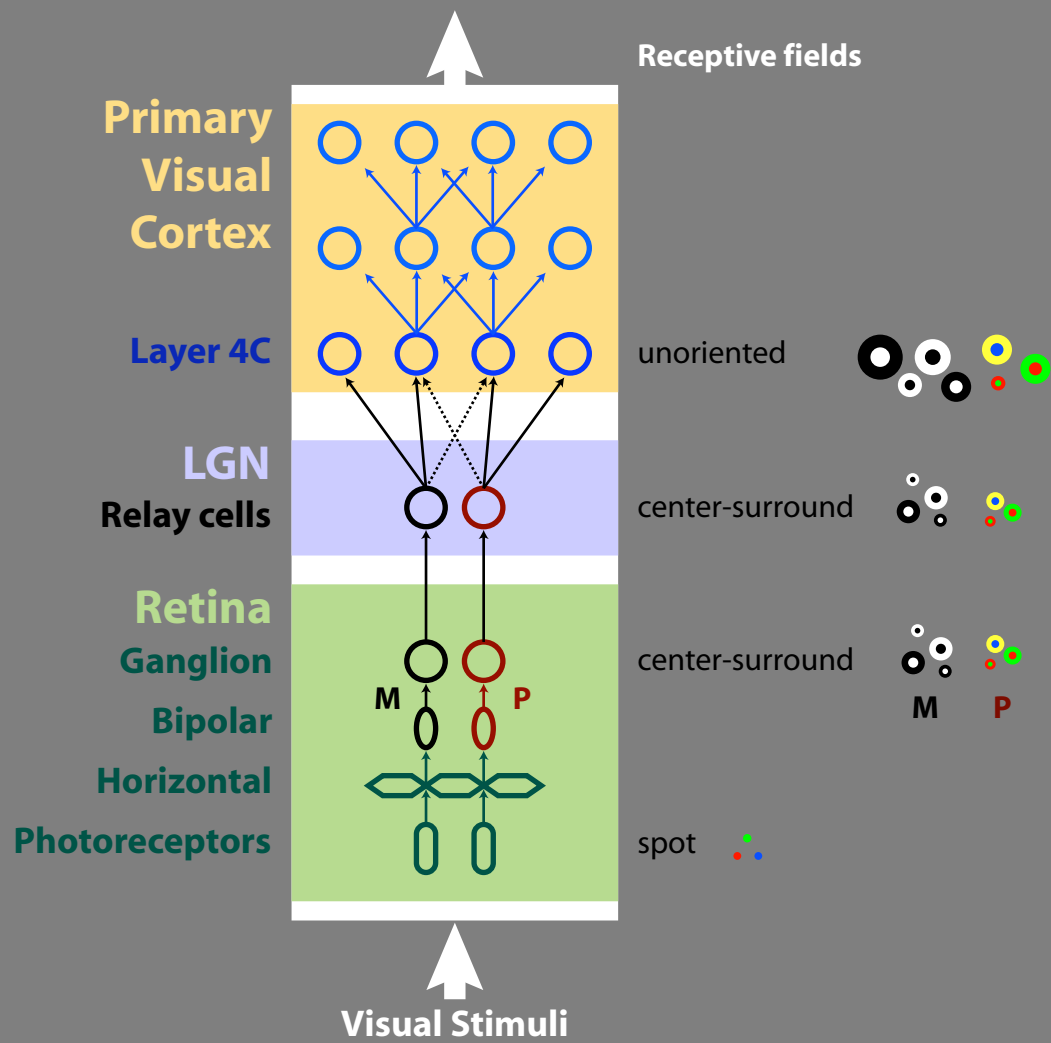
# The visual motion pathway from retina to V1



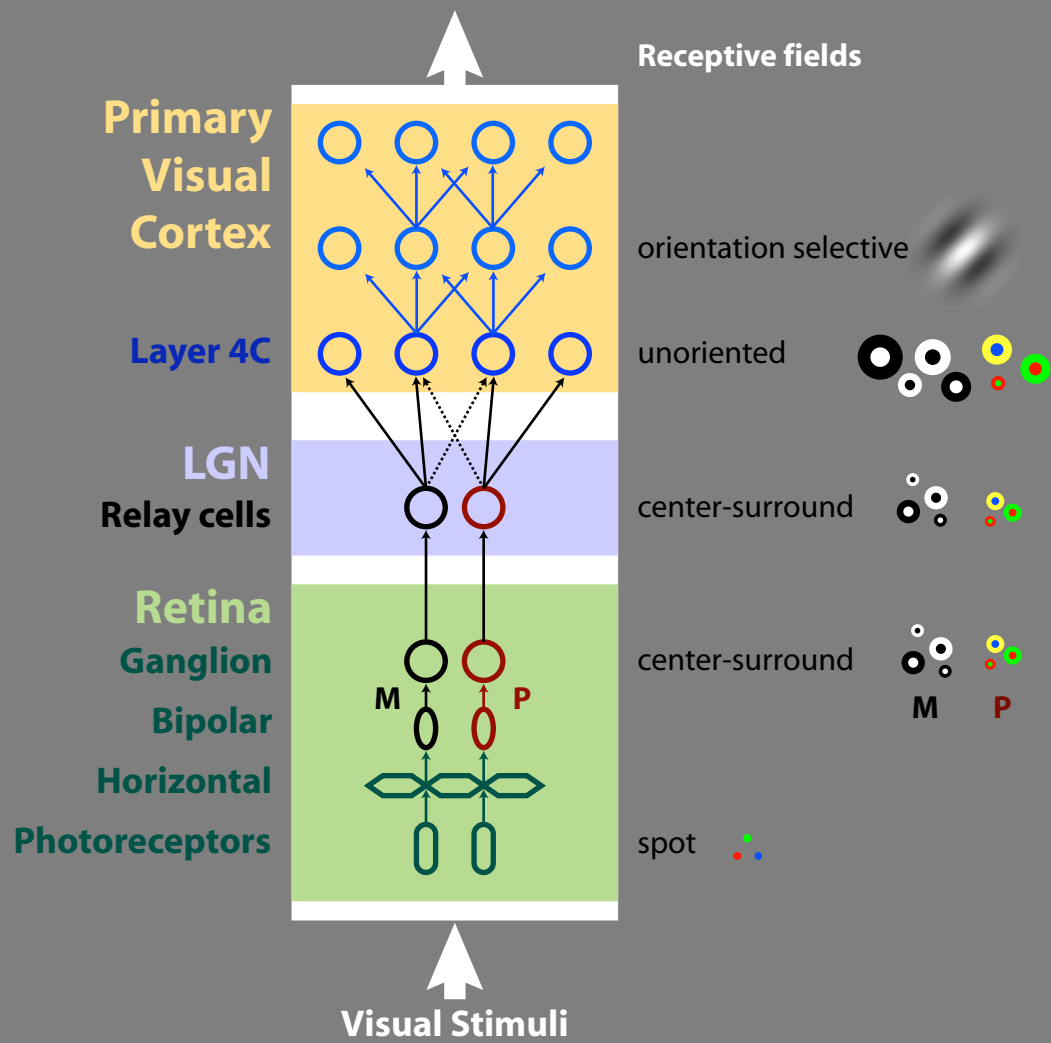
# The visual motion pathway from retina to V1



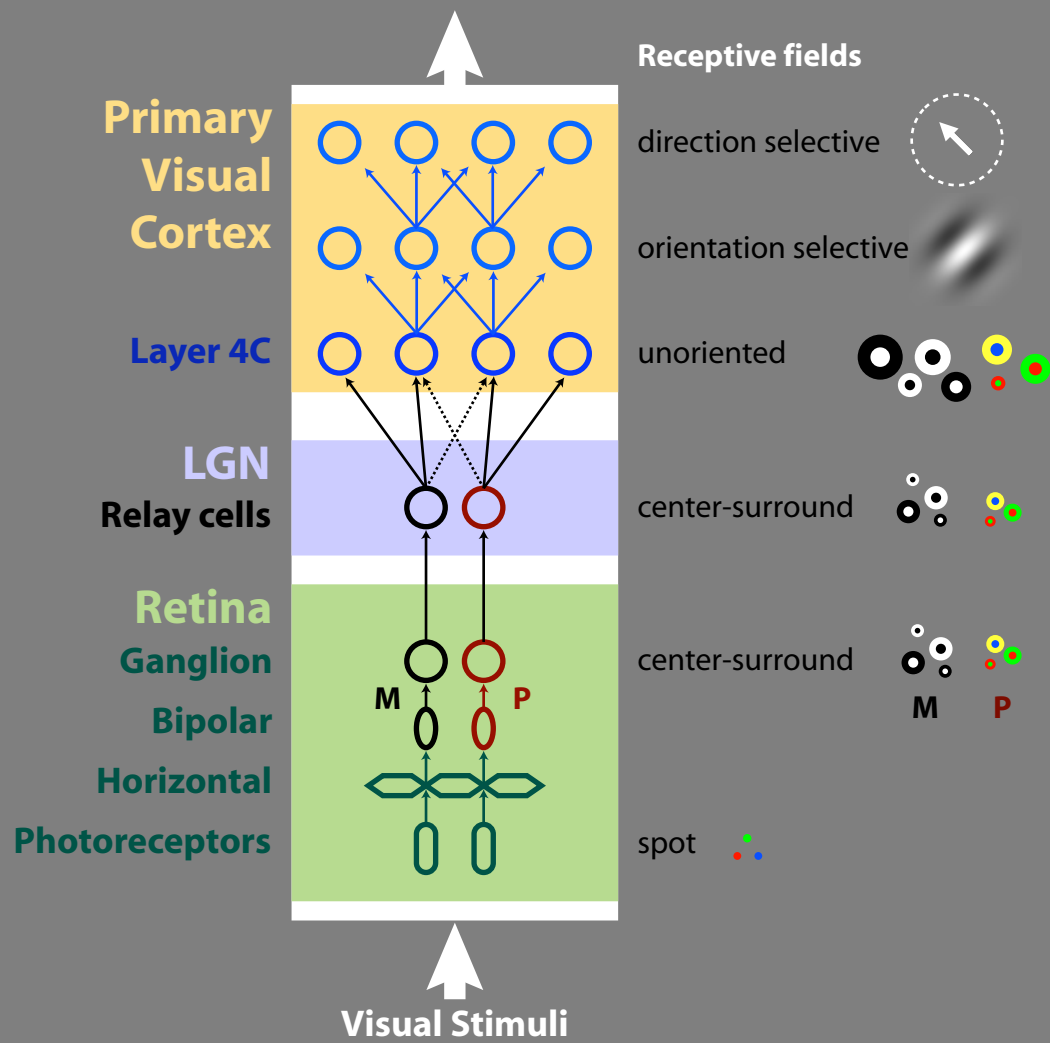
# The visual motion pathway from retina to V1



# The visual motion pathway from retina to V1

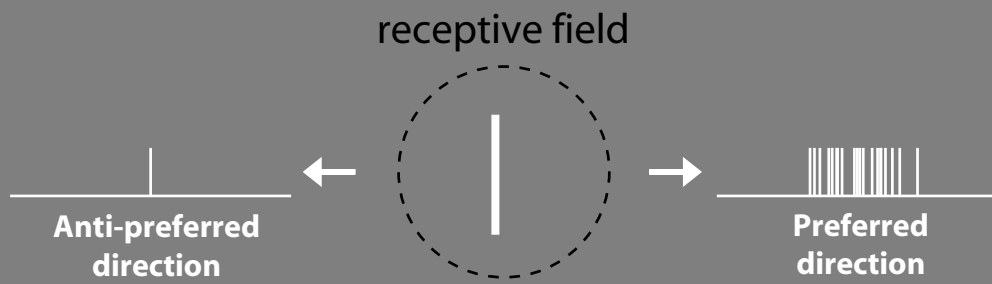


# The visual motion pathway from retina to V1



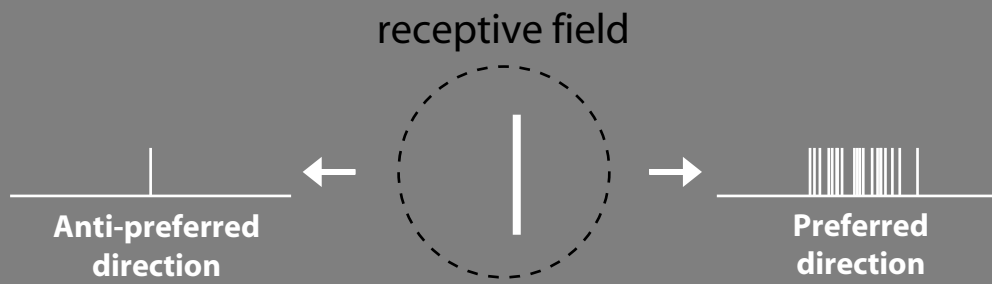
# Direction Selective (DS) Neurons

## V1 complex DS neuron



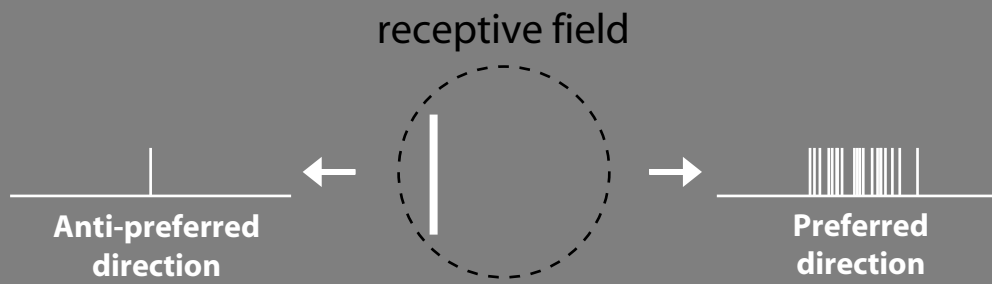
# Direction Selective (DS) Neurons

## V1 complex DS neuron



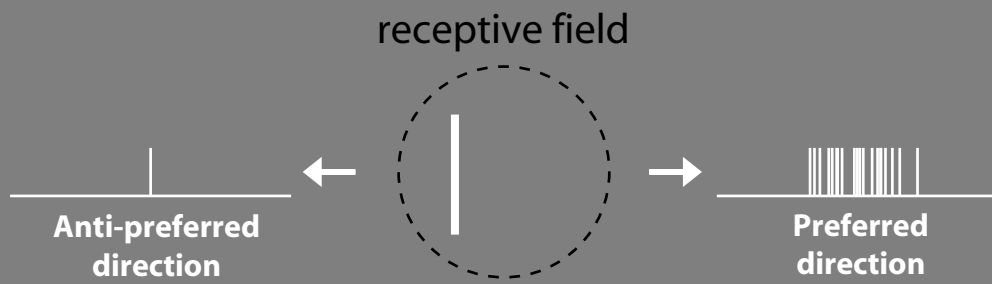
# Direction Selective (DS) Neurons

## V1 complex DS neuron



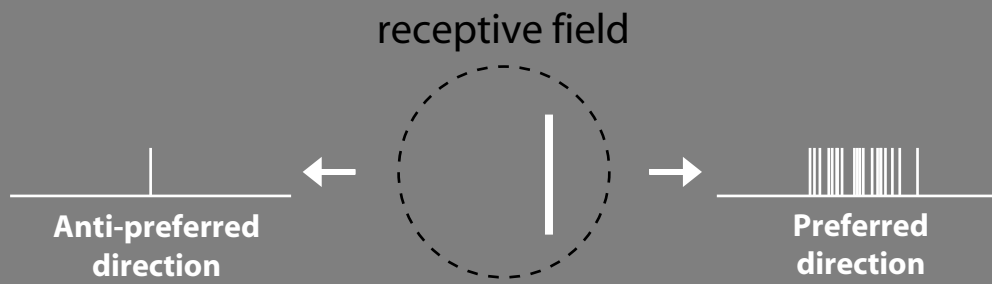
# Direction Selective (DS) Neurons

## V1 complex DS neuron



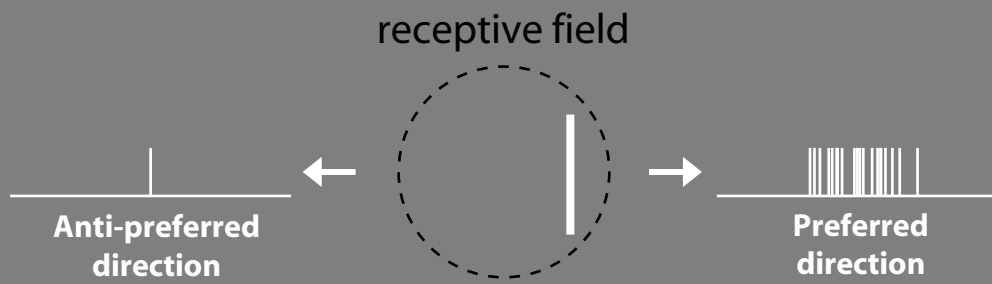
# Direction Selective (DS) Neurons

## V1 complex DS neuron



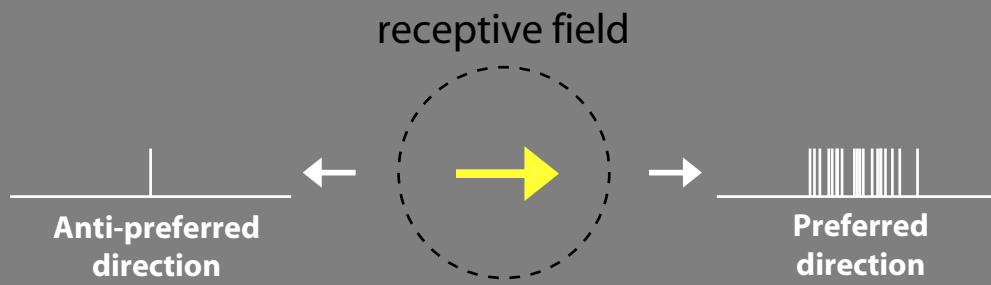
# Direction Selective (DS) Neurons

## V1 complex DS neuron

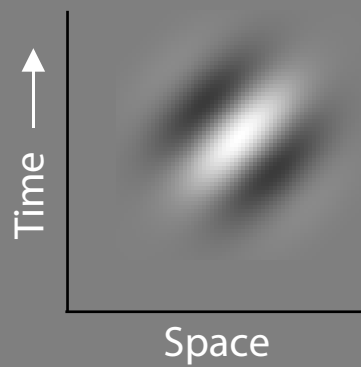


# Direction Selective (DS) Neurons

## V1 complex DS neuron



## Linear filter model

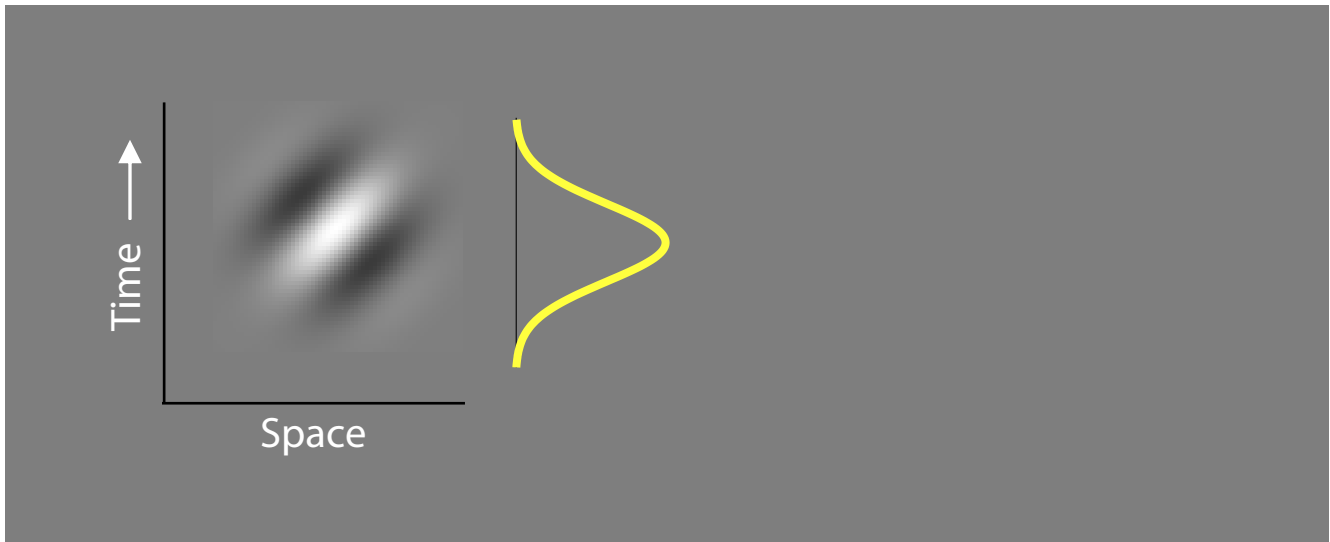


E.g., motion energy (ME) model.

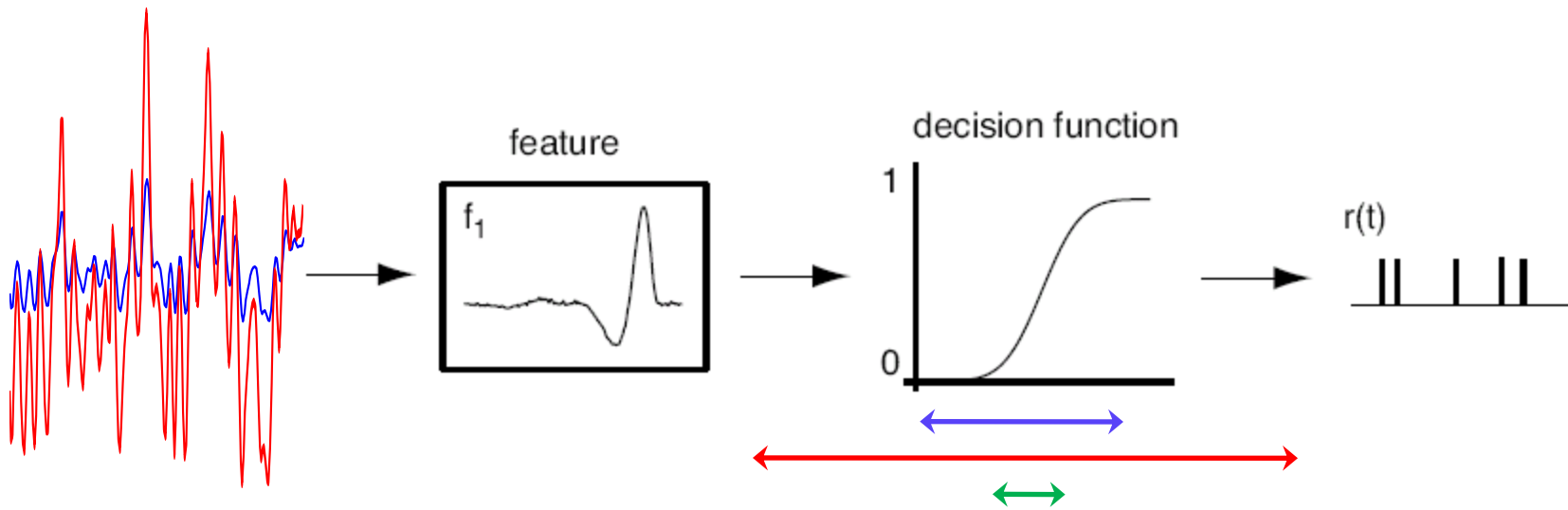
# Temporal integration in visual cortex

## Adaptive temporal integration (ATI)

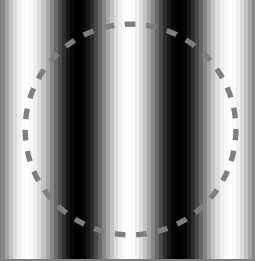
Temporal integration is longer for slower stimulus motion, and shorter for faster motion, as measured in the spike trains of complex DS neurons in V1 and V5/MT (Bair and Movshon, 2004).



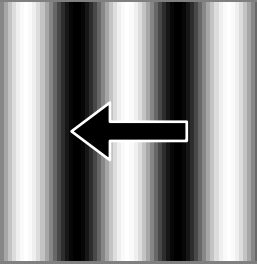
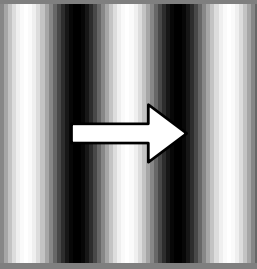
# Adaptive representation of information



As one changes the characteristics of  $s(t)$ , changes can occur both in the *feature* and in the *decision function*

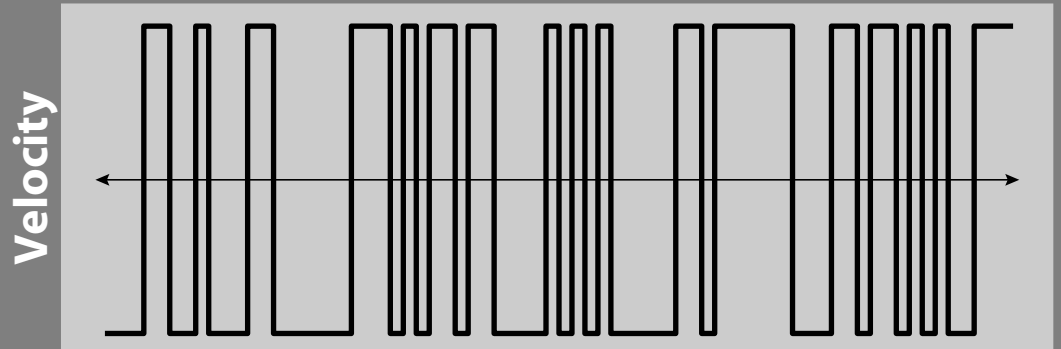


Preferred



Anti-preferred

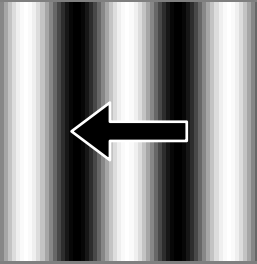
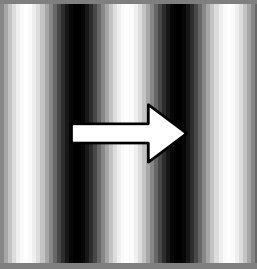
Binary, random motion sequence



Equivalent temporal frequency (TF)

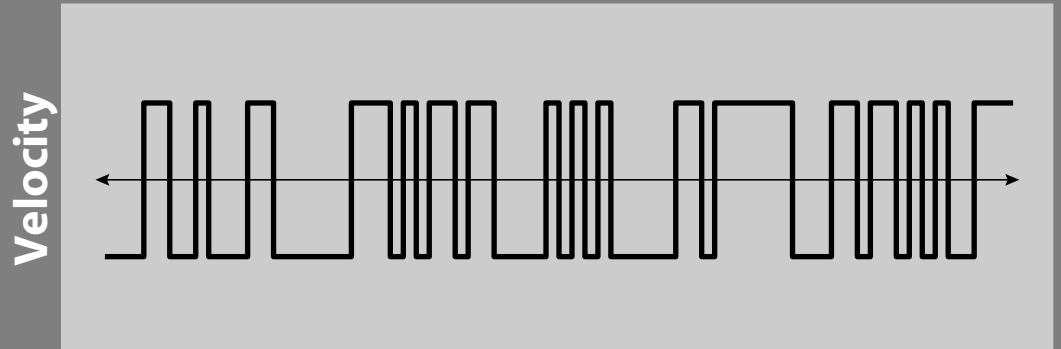
Fastest TF = 25 Hz (1/4 cycle at 100 frames/s)

Preferred



Anti-preferred

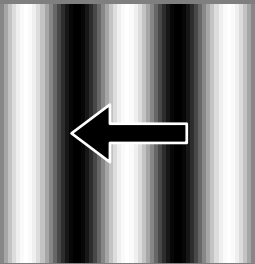
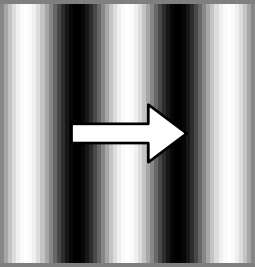
**Binary, random motion sequence**



*Equivalent temporal frequency (TF)*

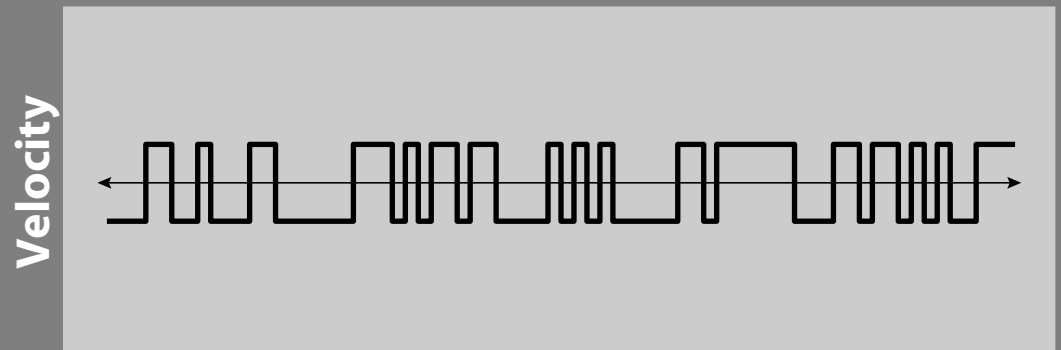
**Fastest TF = 25 Hz** (1/4 cycle at 100 frames/s)

Preferred



Anti-preferred

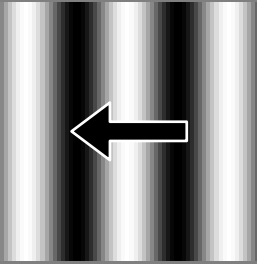
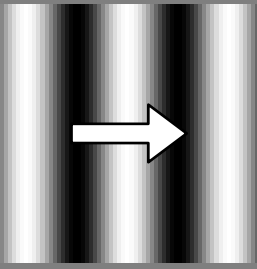
**Binary, random motion sequence**



*Equivalent temporal frequency (TF)*

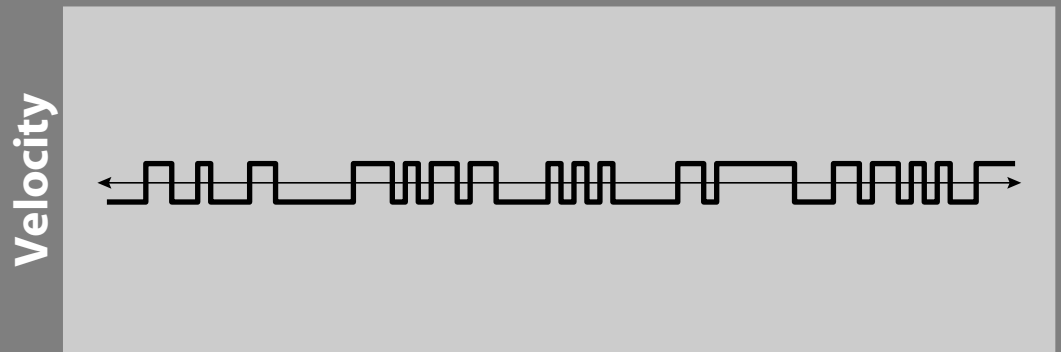
**Fastest TF = 25 Hz** (1/4 cycle at 100 frames/s)

Preferred



Anti-preferred

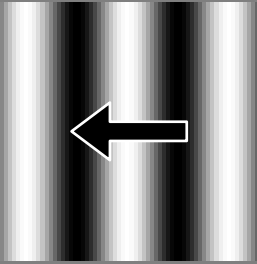
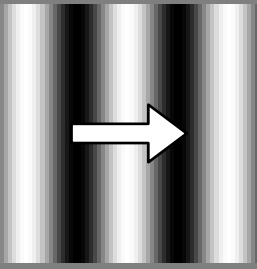
Binary, random motion sequence



*Equivalent temporal frequency (TF)*

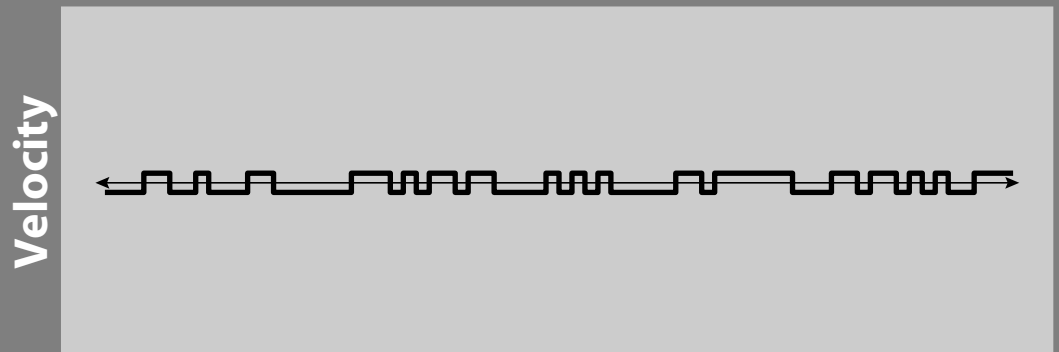
Fastest TF = 25 Hz (1/4 cycle at 100 frames/s)

Preferred



Anti-preferred

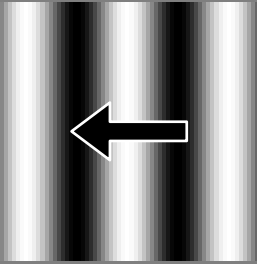
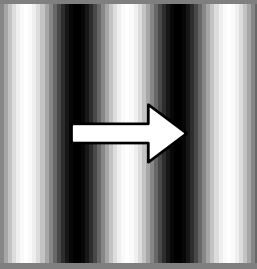
Binary, random motion sequence



*Equivalent temporal frequency (TF)*

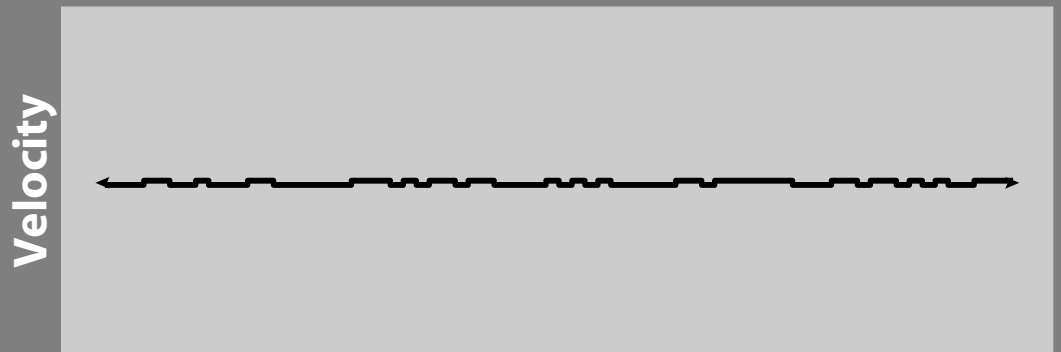
Fastest TF = 25 Hz (1/4 cycle at 100 frames/s)

Preferred



Anti-preferred

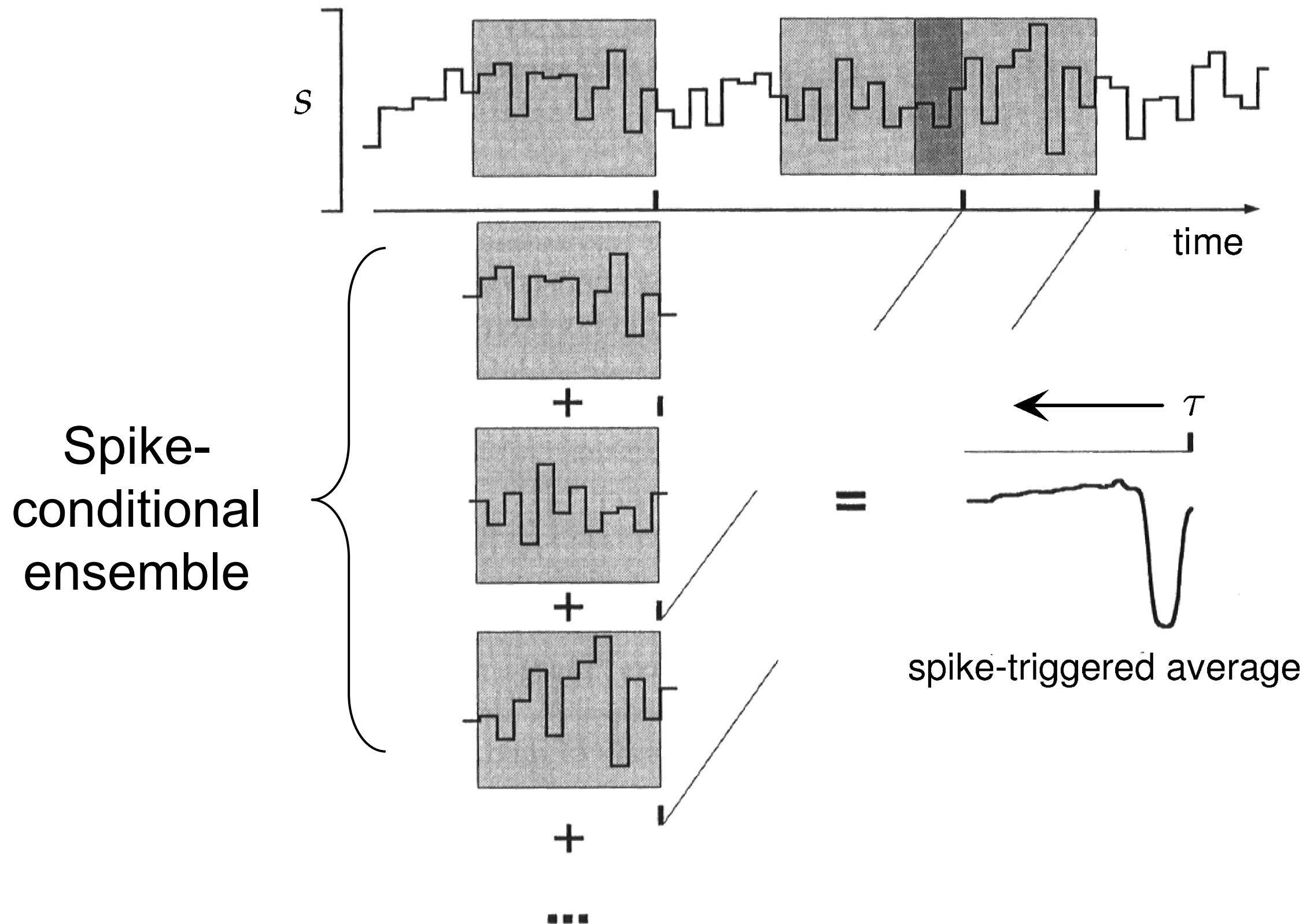
Binary, random motion sequence

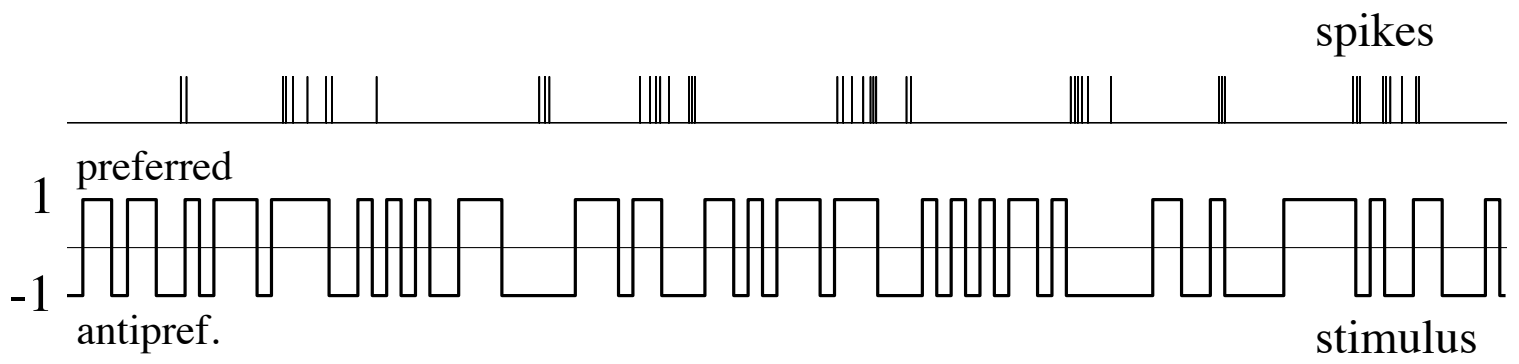


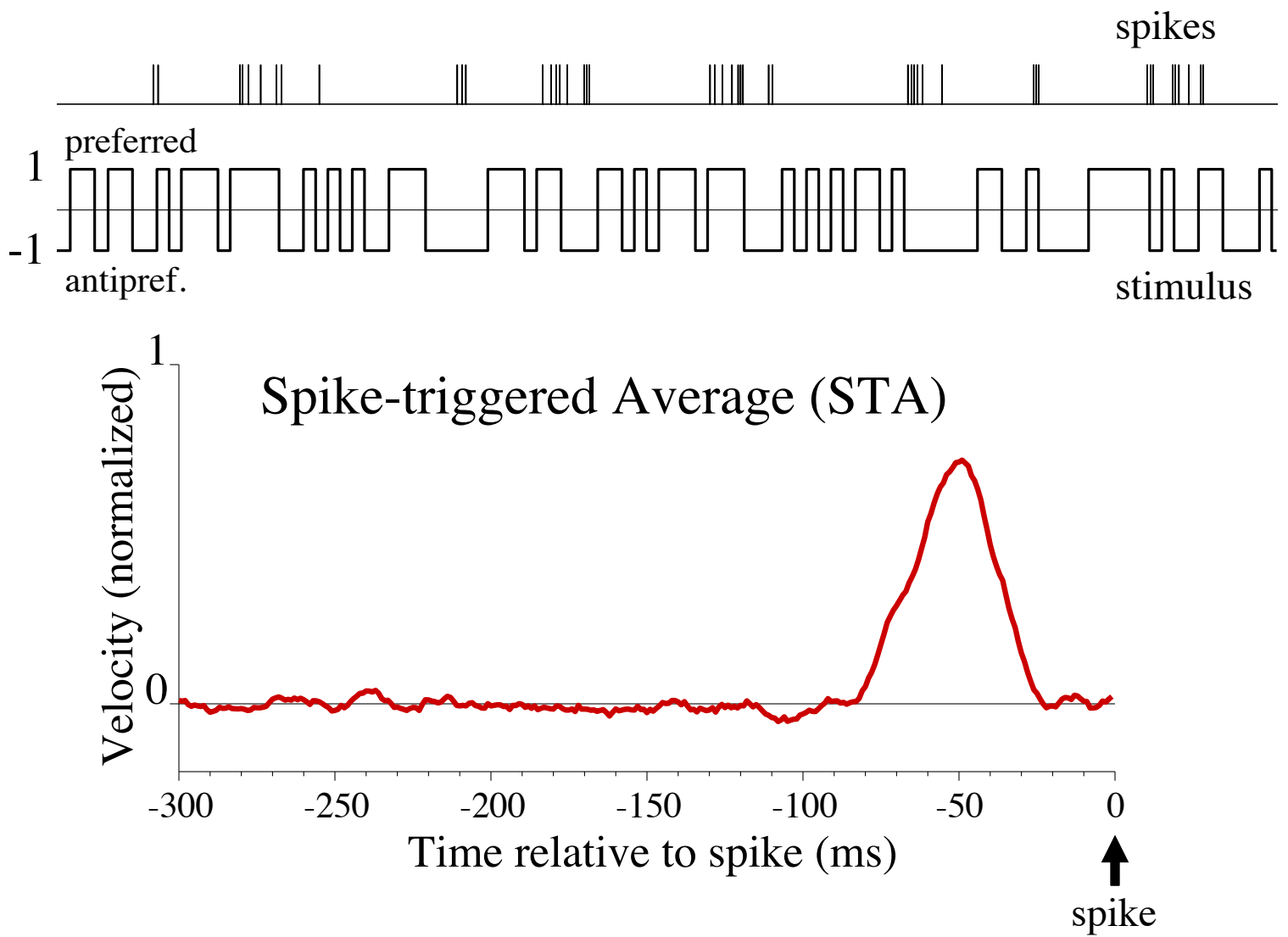
*Equivalent temporal frequency (TF)*

Fastest TF = 25 Hz (1/4 cycle at 100 frames/s)

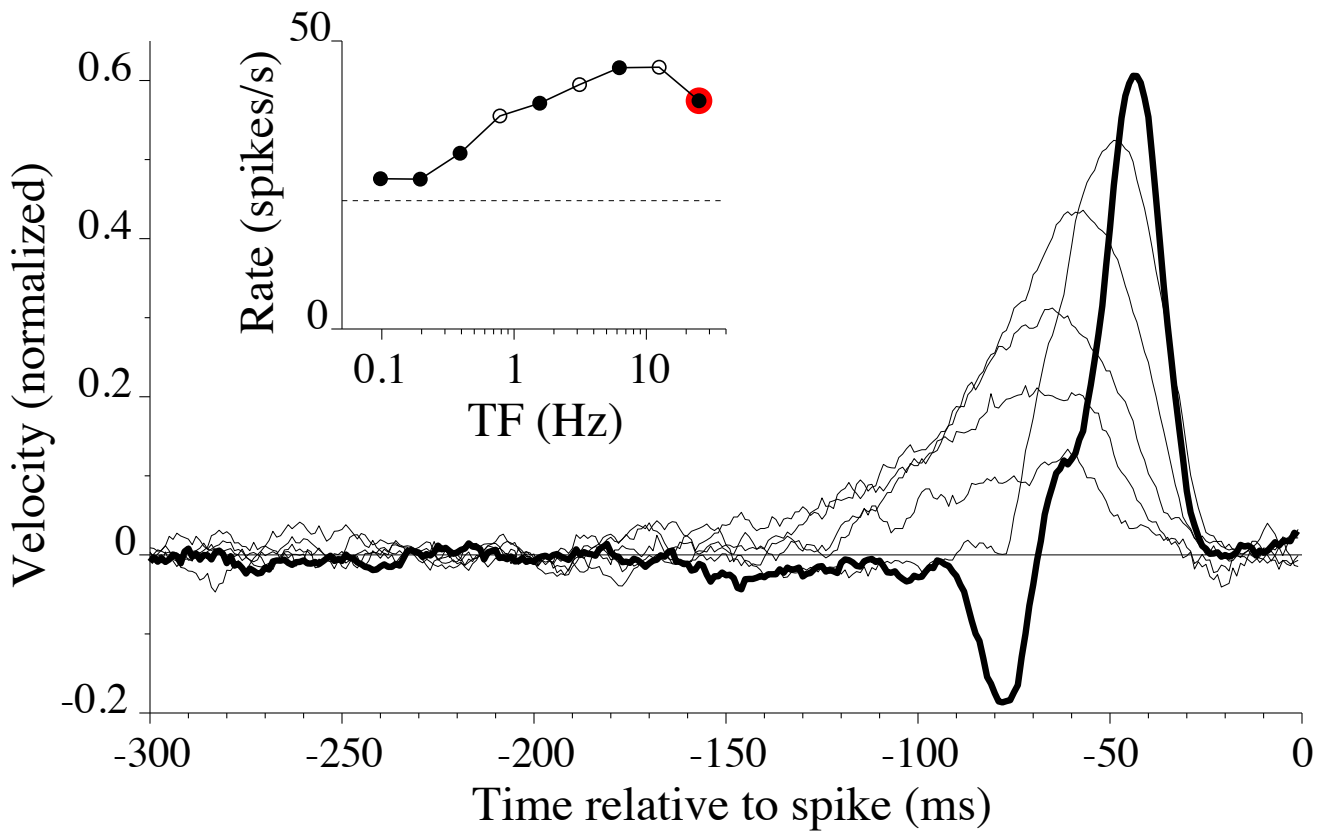
# Reverse correlation: the spike-triggered average



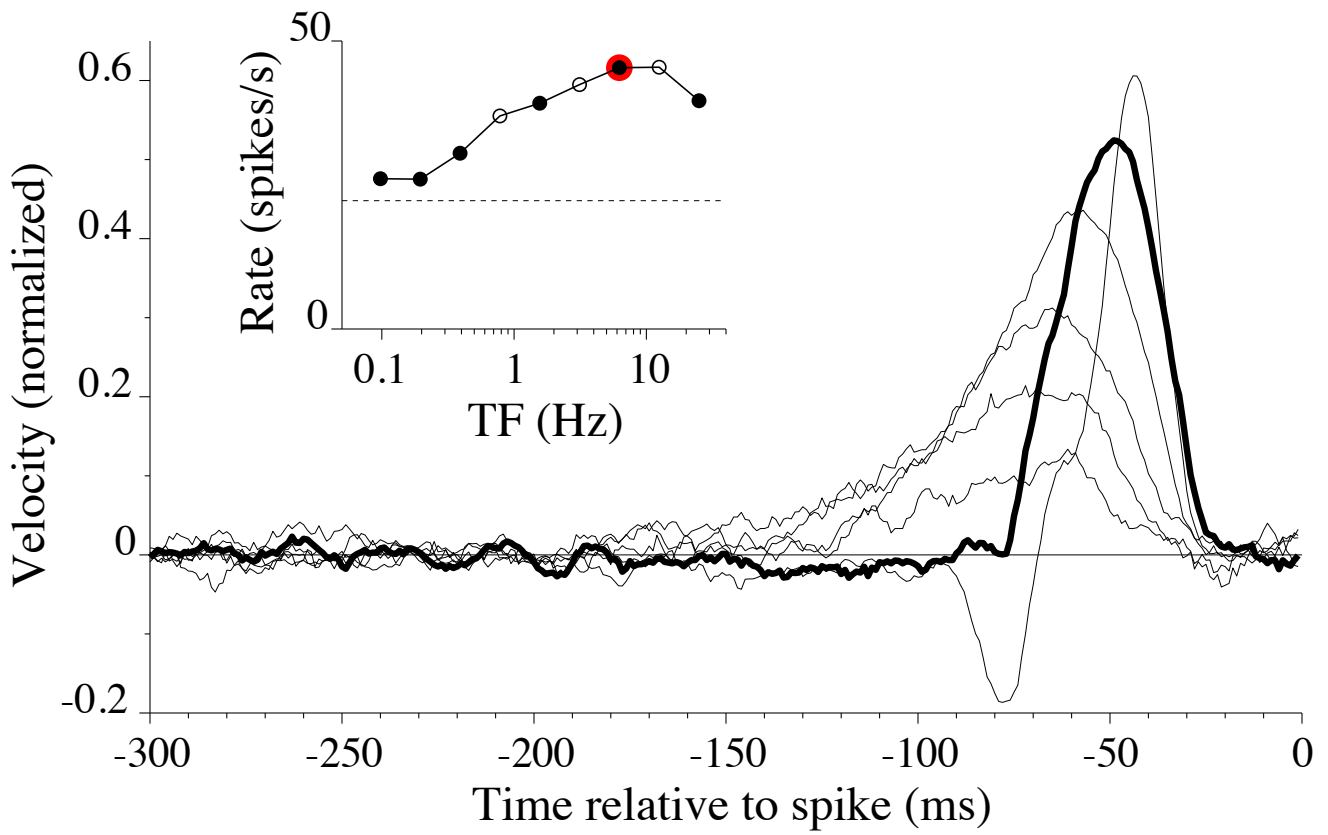




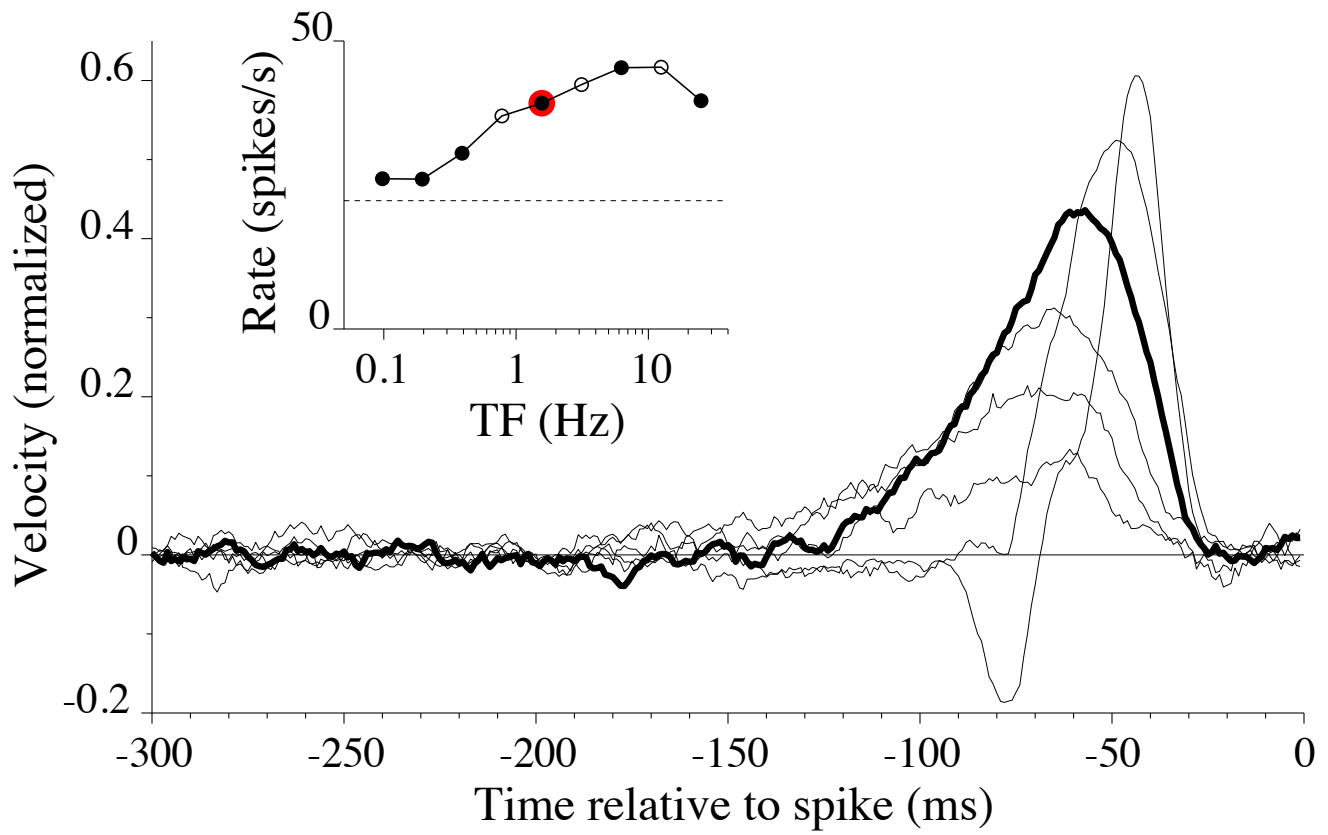
# V1 complex DS cell



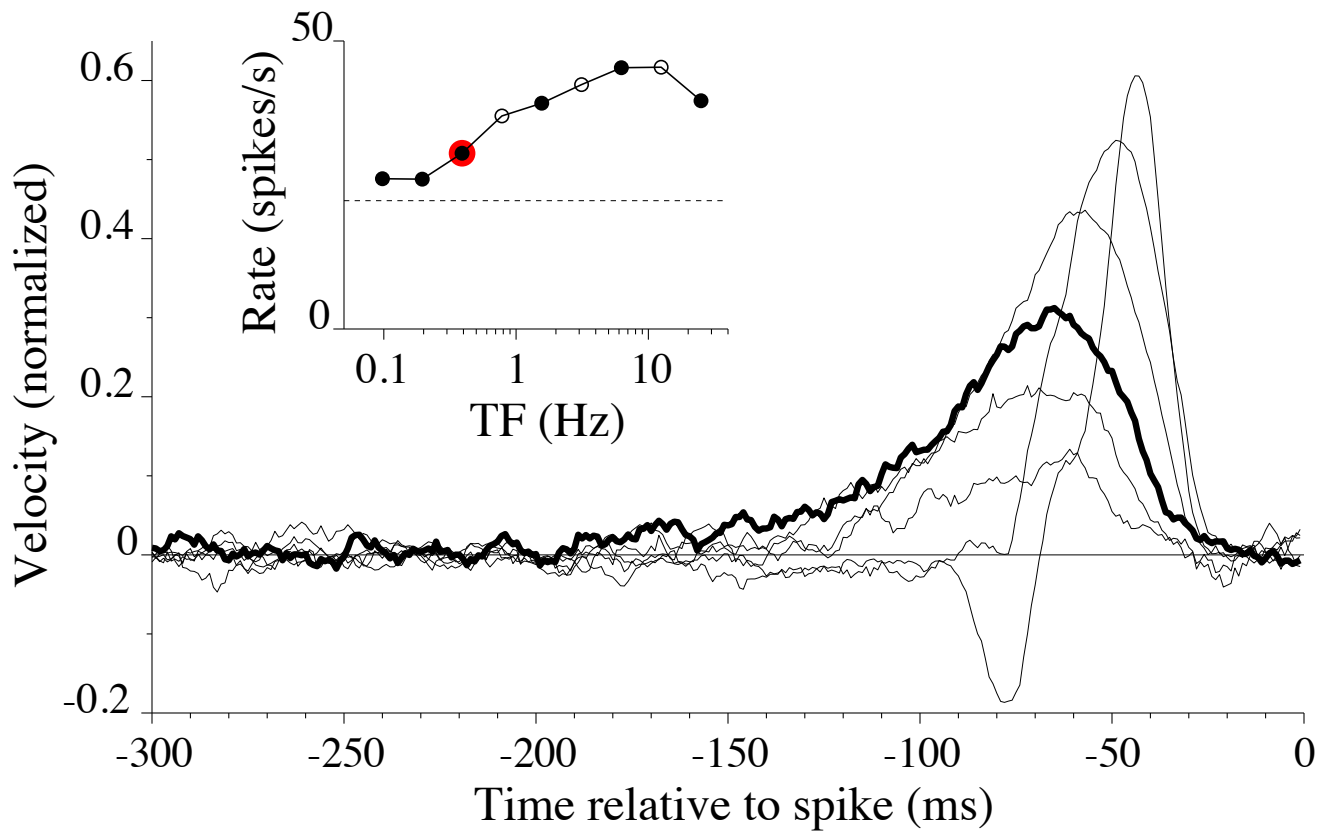
# V1 complex DS cell



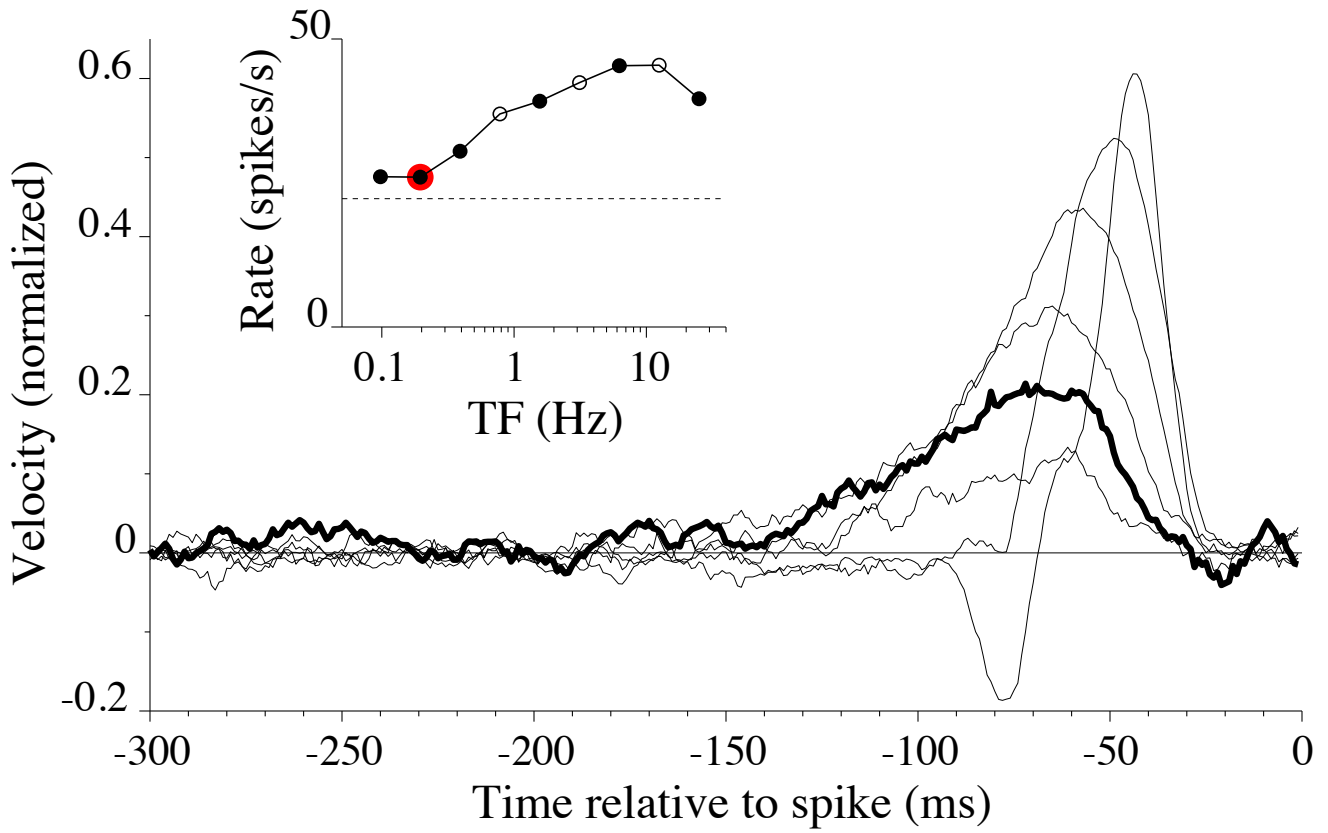
# V1 complex DS cell



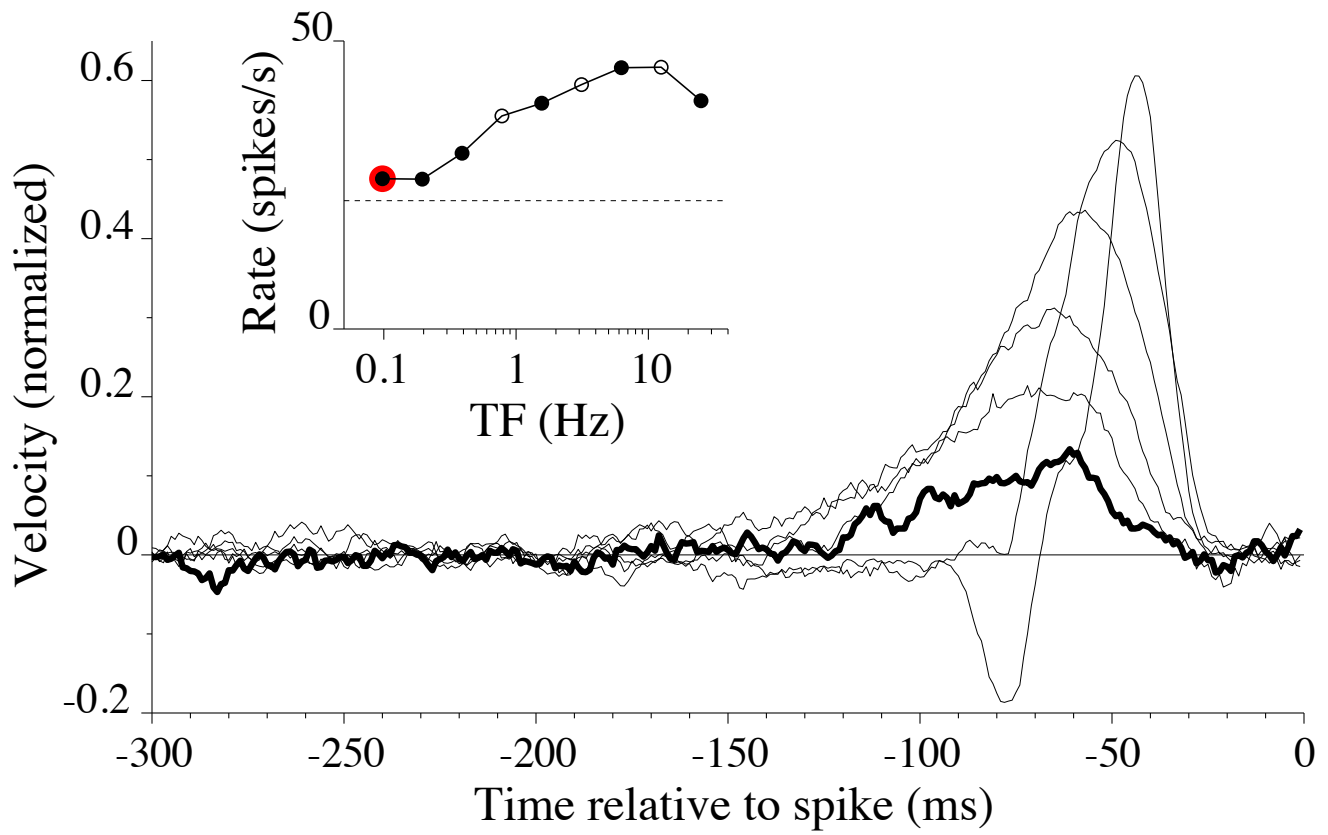
# V1 complex DS cell



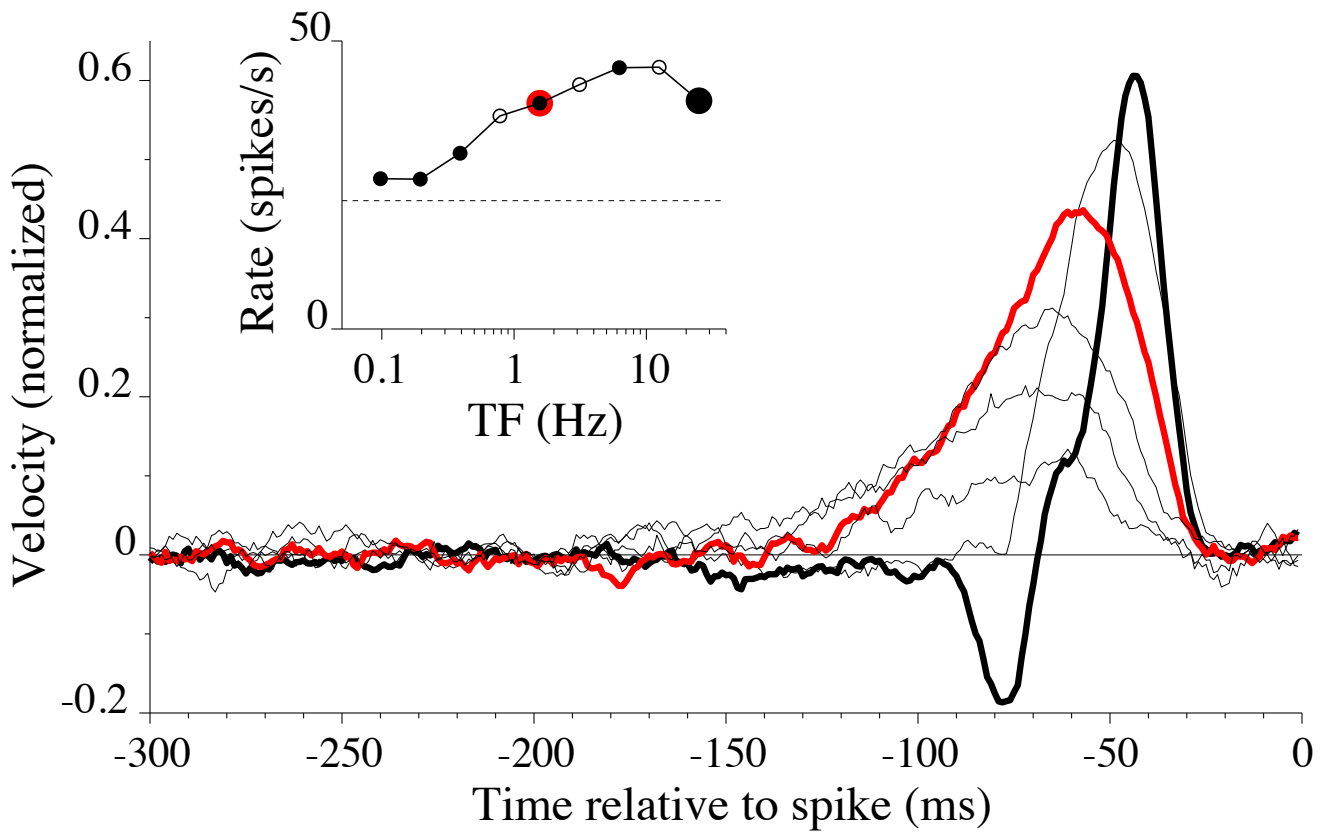
# V1 complex DS cell



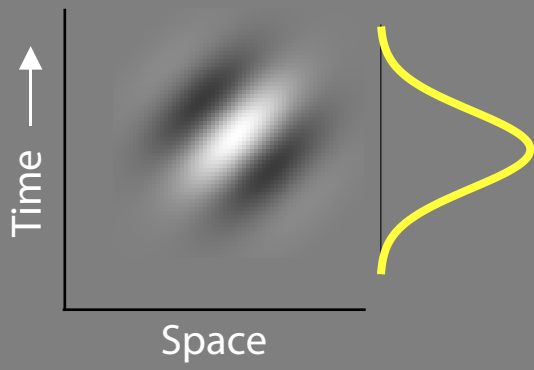
# V1 complex DS cell



# V1 complex DS cell



# Summary of experimental findings



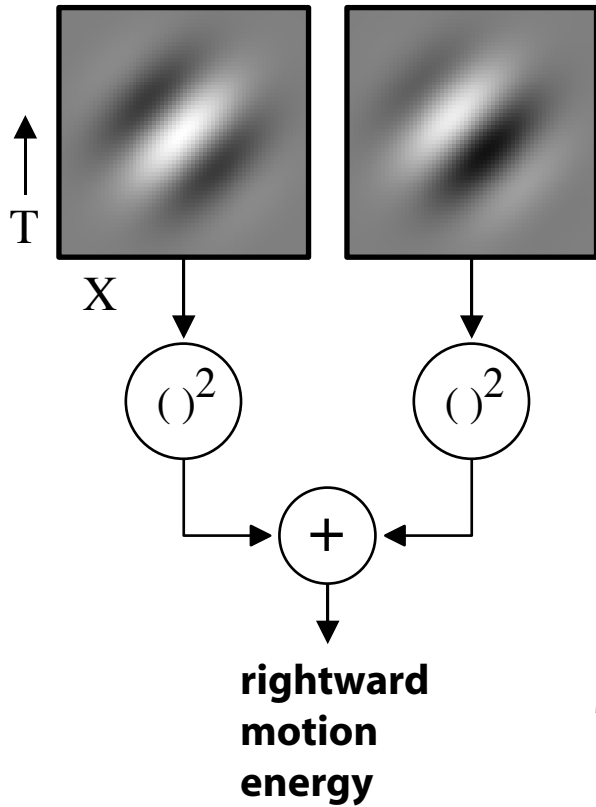
## Summary of experimental findings



### Adaptive temporal integration (ATI)

Temporal integration appears to change with the statistics of the motion (Bair & Movshon, 2004).

# The Motion Energy Model



$$G(\mathbf{r},t) = \frac{1}{(2\pi)^{3/2} \sigma_r^2 \sigma_t} e^{\left(\frac{-|\mathbf{r}|^2}{2\sigma_r^2} - \frac{t^2}{2\sigma_t^2}\right)} e^{-i 2\pi (f_t \mathbf{n} \cdot \mathbf{r} + f_t t)}$$

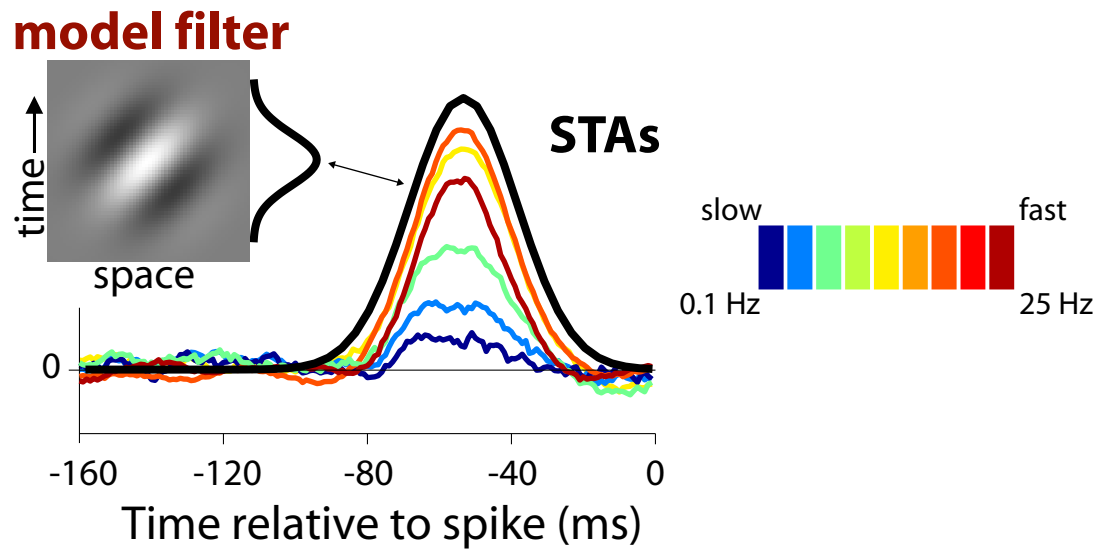
$$\mathbf{n} = (\cos\theta, \sin\theta)$$

$$\mathbf{r} = (x,y)$$

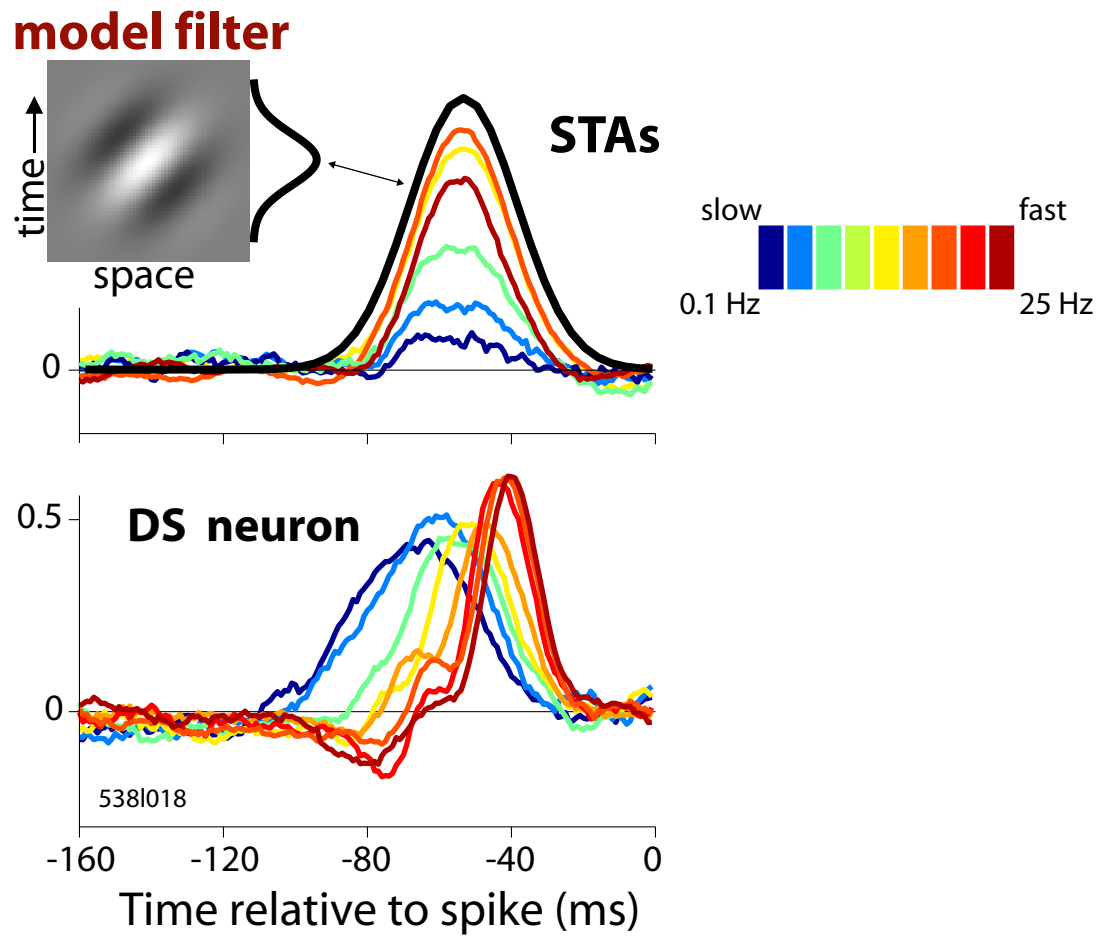
$$ME(\mathbf{r},t) = |G(\mathbf{r},t) * s(\mathbf{r},t)|^2$$

Adelson & Bergen (1985) J Opt Soc Am A

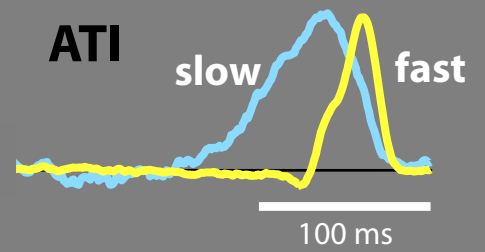
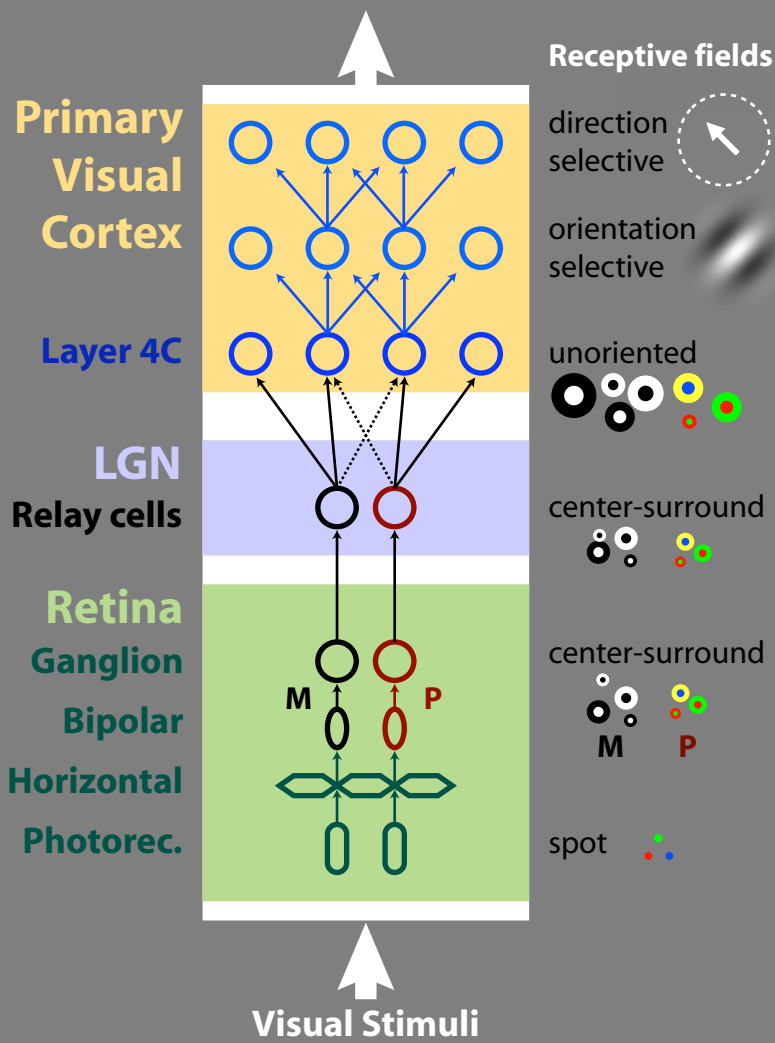
# Temporal Integration in the Motion Energy Model



# Temporal Integration in the Motion Energy Model



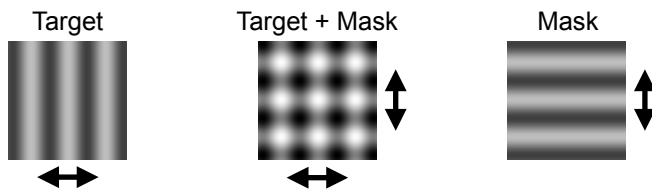
# Visual motion pathway, retina to V1



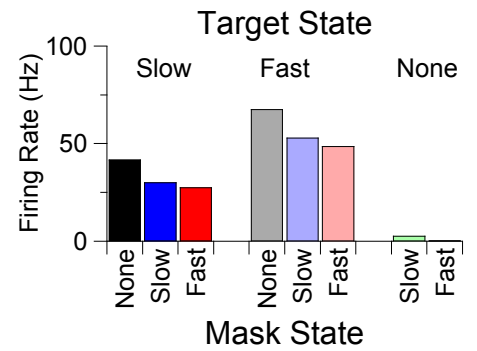
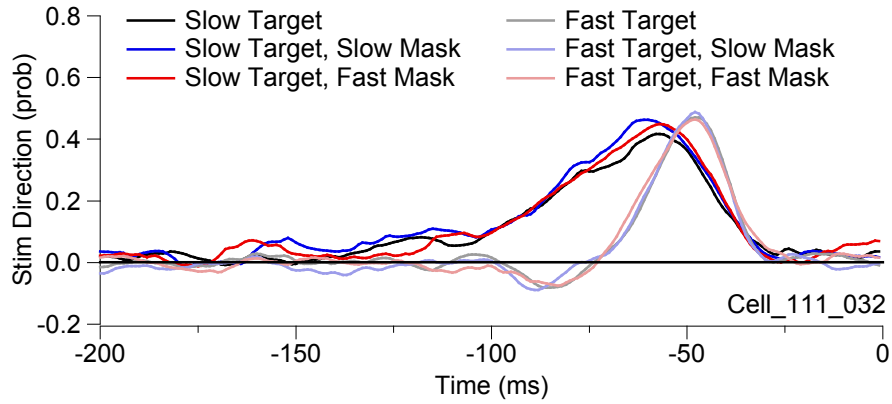
## How could ATI arise?

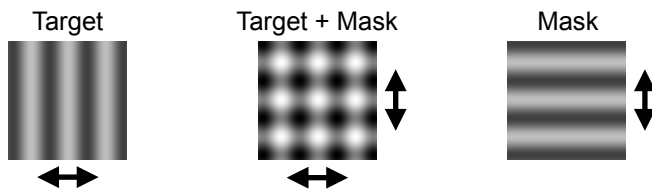
- Changes in the retina
- Cortical normalization
- Adaptation at the soma
- Non-linear interaction at spike generation
- Parallel pathways: convergence of fast and slow channels

## Mask Stimulus

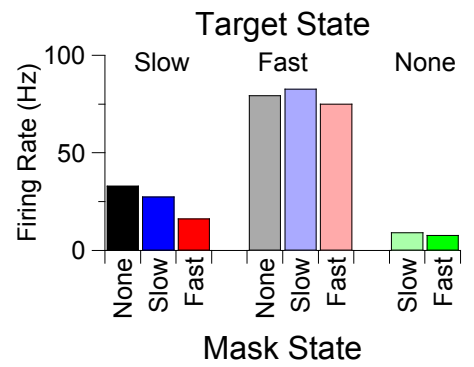
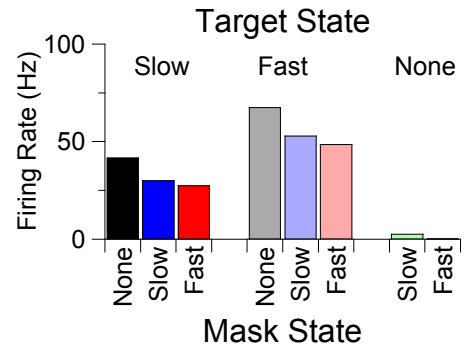
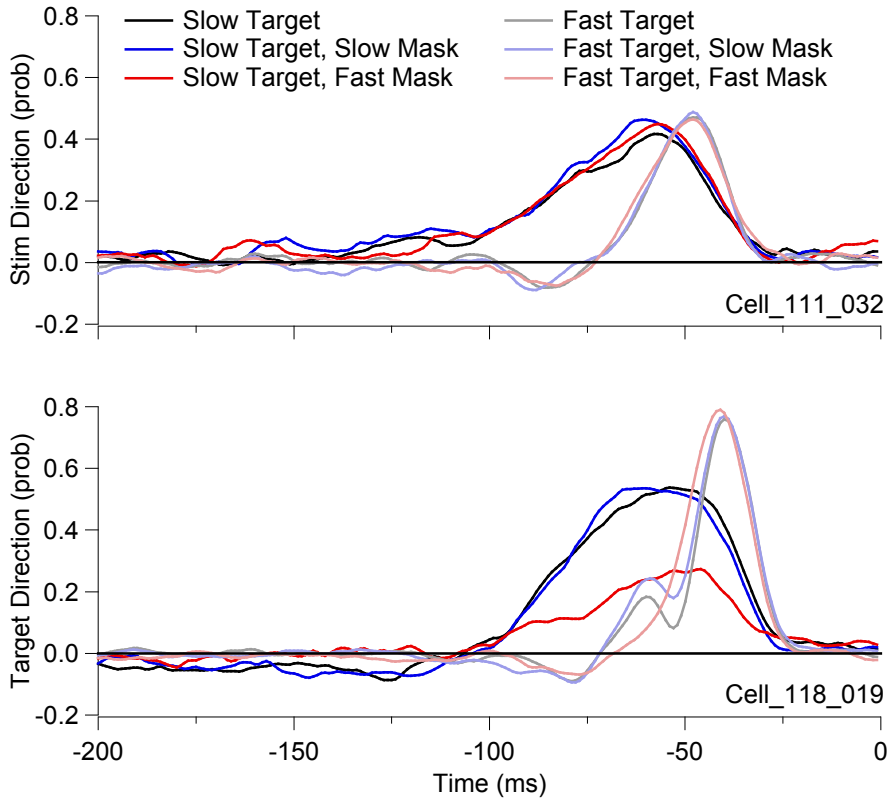


# Results for one V1 complex DS cell

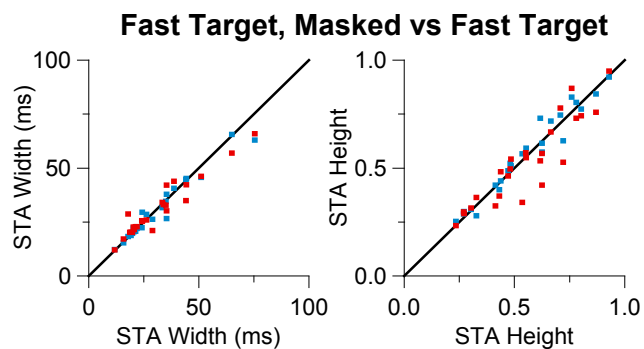
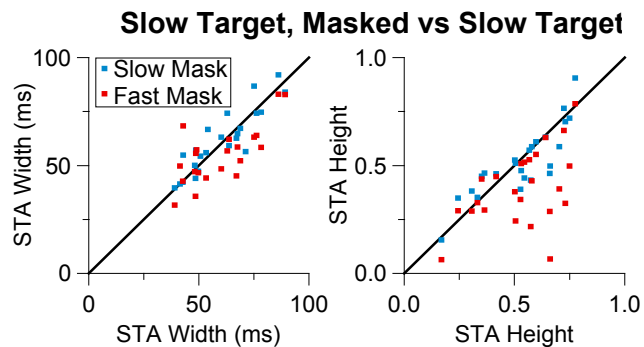
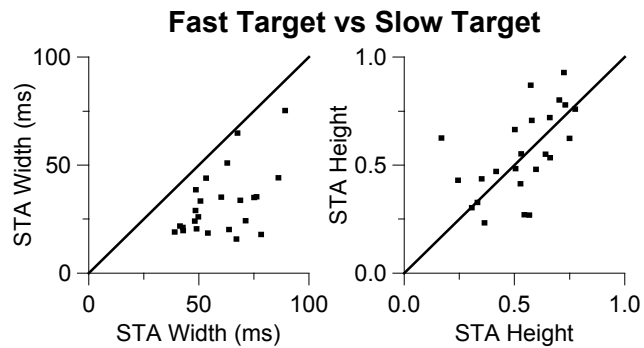
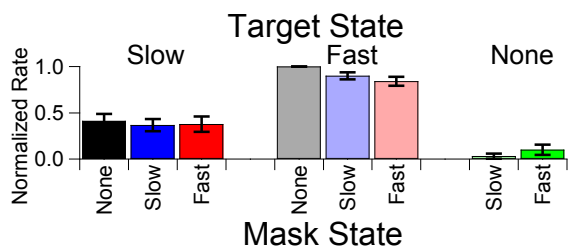




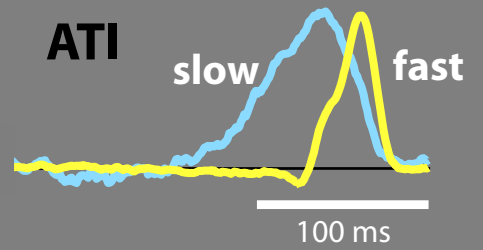
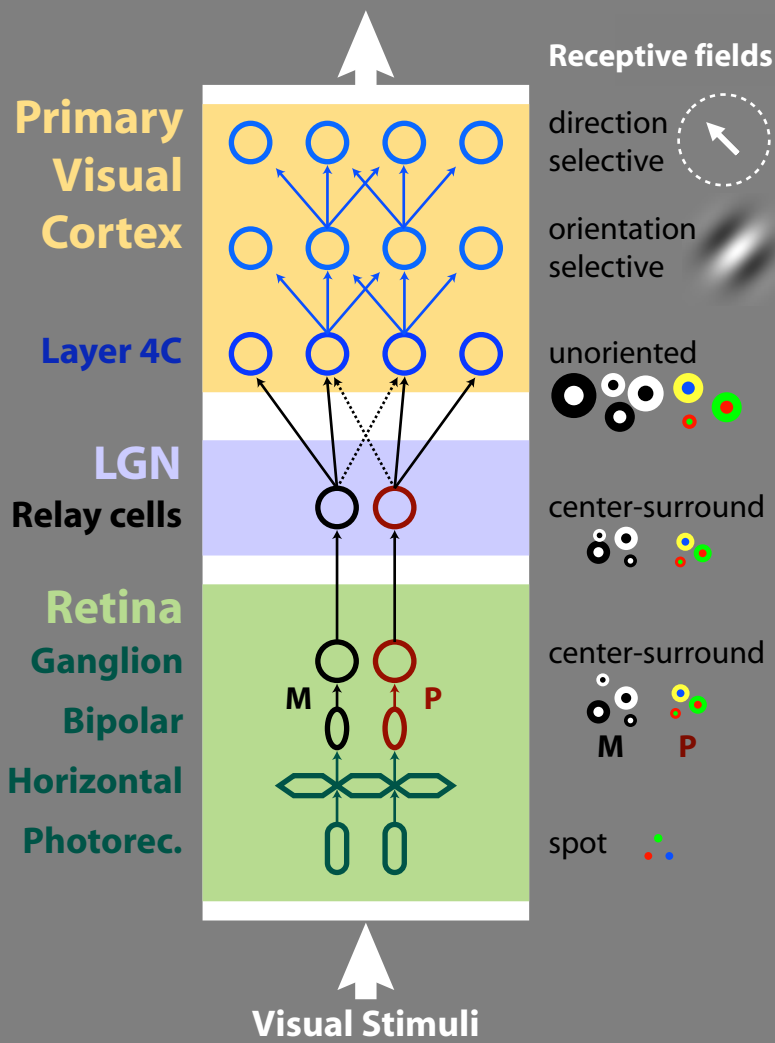
# Results for two V1 complex DS cells



# Database Summary



# Visual motion pathway, retina to V1



## How could ATI arise?

- X-** Changes in the retina
- X-** Cortical normalization
- Adaptation at the soma
- Non-linear interaction at spike generation
- Parallel pathways: convergence of fast and slow channels

**ATI is channel specific.**



## Noise-driven adaptation: in vitro and mathematical analysis<sup>☆</sup>

Liam Paninski<sup>\*,1</sup>, Brian Lau, Alex Reyes

*Center for Neural Science, New York University, 4 Washington Place, New York, NY 10003, USA*

---

### Abstract

Variance adaptation processes have recently been examined in cells of the fly visual system and various vertebrate preparations. To better understand the contributions of somatic mechanisms to this kind of adaptation, we recorded intracellularly in vitro from neurons of rat sensorimotor cortex. The cells were stimulated with a noise current whose standard deviation was varied parametrically. We observed systematic variance-dependent adaptation (defined as a scaling of a nonlinear transfer function) similar in many respects to the effects observed in vivo. The fact that similar adaptive phenomena are seen in such different preparations led us to investigate a simple model of stochastic stimulus-driven neural activity. The simplest such model, the leaky integrate-and-fire (LIF) cell driven by noise current, permits us to analytically compute many quantities relevant to our observations on adaptation. We show that the LIF model displays “adaptive” behavior which is quite similar to the effects observed in vivo and in vitro.

© 2003 Elsevier Science B.V. All rights reserved.

*Keywords:* Adaptation; Noise; Integrate-and-fire; Fokker–Planck

---

It is widely understood that sensory neurons adapt to the prevailing statistics of their inputs [10]. Fairhall et al. [5] recently reported one such adaptation process in the fly visual system; they described a motion-sensitive neuron that appears to scale its input–output function to adapt its firing rate to the variance of the observed motion signal. However, the mechanisms underlying this type of contrast-dependent adaptation are unknown; specifically, it is unclear whether the observed phenomena arise from network

---

<sup>☆</sup> This work was supported by NSF Grant IBN-0079619. LP and BL are supported by HHMI and NDSEG predoctoral fellowships, respectively. We thank E. Simoncelli for many interesting discussions.

\* Corresponding author.

*E-mail address:* [liam@cns.nyu.edu](mailto:liam@cns.nyu.edu) (L. Paninski).

<sup>1</sup> Contact: [liam@cns.nyu.edu](mailto:liam@cns.nyu.edu); <http://www.cns.nyu.edu/~liam>

# Intrinsic Gain Modulation and Adaptive Neural Coding

Sungho Hong<sup>1\*</sup>, Brian Nils Lundstrom, Adrienne L. Fairhall

Physiology and Biophysics Department, University of Washington, Seattle, Washington, United States of America

## Abstract

In many cases, the computation of a neural system can be reduced to a receptive field, or a set of linear filters, and a thresholding function, or gain curve, which determines the firing probability; this is known as a linear/nonlinear model. In some forms of sensory adaptation, these linear filters and gain curve adjust very rapidly to changes in the variance of a randomly varying driving input. An apparently similar but previously unrelated issue is the observation of gain control by background noise in cortical neurons: the slope of the firing rate versus current ( $f-I$ ) curve changes with the variance of background random input. Here, we show a direct correspondence between these two observations by relating variance-dependent changes in the gain of  $f-I$  curves to characteristics of the changing empirical linear/nonlinear model obtained by sampling. In the case that the underlying system is fixed, we derive relationships relating the change of the gain with respect to both mean and variance with the receptive fields derived from reverse correlation on a white noise stimulus. Using two conductance-based model neurons that display distinct gain modulation properties through a simple change in parameters, we show that coding properties of both these models quantitatively satisfy the predicted relationships. Our results describe how both variance-dependent gain modulation and adaptive neural computation result from intrinsic nonlinearity.

**Citation:** Hong S, Lundstrom BN, Fairhall AL (2008) Intrinsic Gain Modulation and Adaptive Neural Coding. *PLoS Comput Biol* 4(7): e1000119. doi:10.1371/journal.pcbi.1000119

**Editor:** Karl J. Friston, University College London, United Kingdom

**Received:** January 30, 2008; **Accepted:** June 9, 2008; **Published:** July 18, 2008

**Copyright:** © 2008 Hong et al. This is an open-access article distributed under the terms of the Creative Commons Attribution License, which permits unrestricted use, distribution, and reproduction in any medium, provided the original author and source are credited.

**Funding:** This work was supported by a Burroughs-Wellcome Careers at the Scientific Interface grant, a Sloan Research Fellowship, and a McKnight Scholar Award to ALF. BNL was supported by grant number F30NS055650 from the National Institute of Neurological Disorders and Stroke, the Medical Scientist Training Program at the University of Washington supported by the National Institute of General Sciences, and an Achievement Rewards for College Scientists fellowship.

**Competing Interests:** The authors have declared that no competing interests exist.

\* E-mail: shhong@oist.jp

† Current address: Computational Neuroscience Unit, Okinawa Institute of Science and Technology, Onna-son, Okinawa, Japan

## Introduction

An  $f-I$  curve, defined as the mean firing rate in response to a stationary mean current input, is one of the simplest ways to characterize how a neuron transforms a stimulus into a spike train output as a function of the magnitude of a single stimulus parameter. Recently, the dependence of  $f-I$  curves on other input statistics such as the variance has been examined: the slope of the  $f-I$  curve, or gain, is modulated in diverse ways in response to different intensities of added noise [1–4]. This enables multiplicative control of the neuronal gain by the level of background synaptic activity [1]: changing the level of the background synaptic activity is equivalent to changing the variance of the noisy balanced excitatory and inhibitory input current to the soma, which modulates the gain of the  $f-I$  curve. It has been demonstrated that such somatic gain modulation, combined with saturation in the dendrites, can lead to multiplicative gain control in a single neuron by background inputs [5]. From a computational perspective, the sensitivity of the firing rate to mean or variance can be thought of as distinguishing the neuron's function as either an integrator (greater sensitivity to the mean) or a differentiator/coincidence detector (greater sensitivity to fluctuations, as quantified by the variance) [3,6,7].

An alternative method of characterizing a neuron's input-to-output transformation is through a linear/nonlinear (LN) cascade model [8,9]. These models comprise a set of linear filters or receptive field that selects particular features from the input; the filter output is transformed by a nonlinear threshold stage into a time-varying firing rate. Spike-triggered covariance analysis

[10,11] reconstructs a model with multiple features from a neuron's input/output data. It has been widely employed to characterize both neural systems [12–15] and single neurons or neuron models subject to current or conductance inputs [16–19].

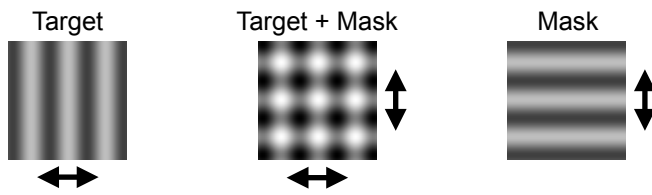
Generally, results of reverse correlation analysis may depend on the statistics of the stimulus used to sample the model [15,19–25]. While some of the dependence on stimulus statistics in the response of a neuron or neural system may reflect underlying plasticity, in some cases, the rapid timescale of the changes suggests the action of intrinsic nonlinearities in systems with *fixed* parameters [16,19,25–29], which changes the *effective* computation of a neuron.

Our goal here is to unify the  $f-I$  curve description of variance-dependent adaptive computation with that given by the LN model: we present analytical results showing that the variance-dependent modulation of the firing rate is closely related to adaptive changes in the *recovered* LN model if a fixed underlying model is assumed. When the model relies only on a single feature, we find that such a system can show only a single type of gain modulation, which accompanies an interesting asymptotic scaling behavior. With multiple features, the model can show more diverse adaptive behaviors, exemplified by two conductance-based models that we will study.

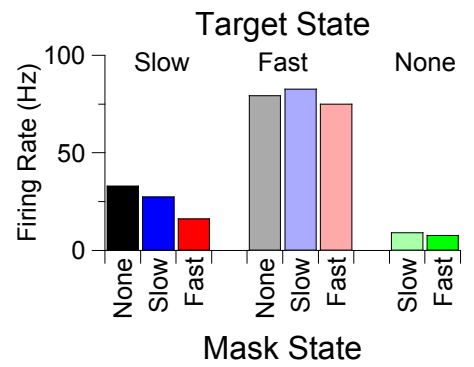
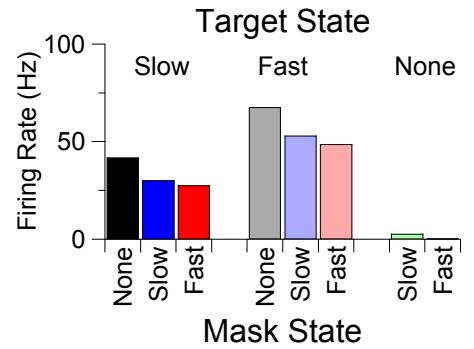
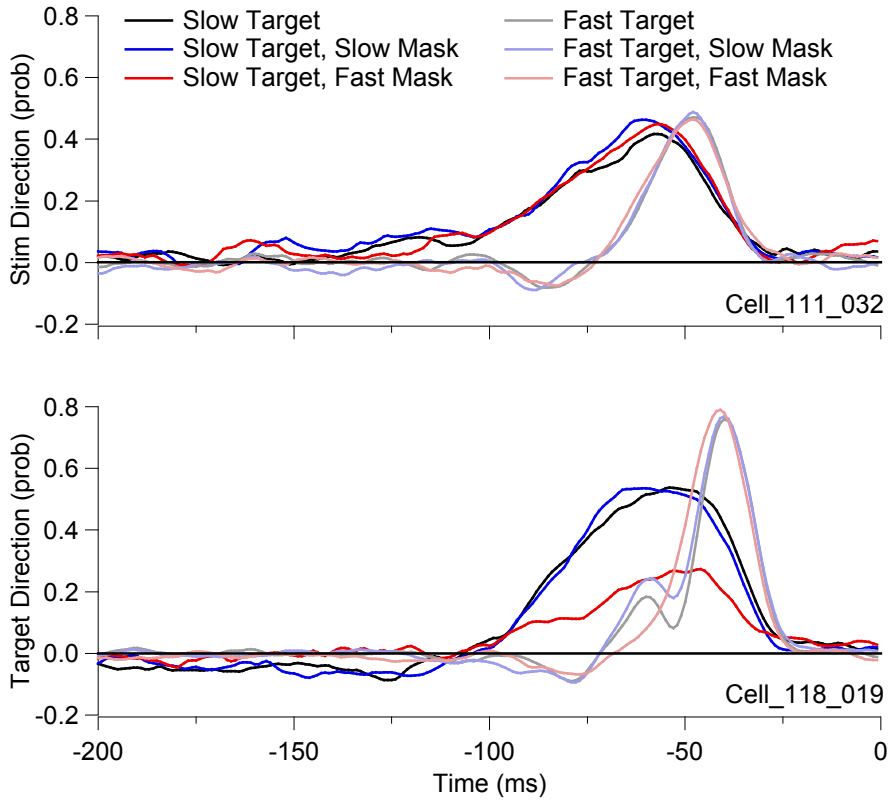
## Results

### Diverse Variance-Dependent Gain Modulations without Spike Rate Adaptation

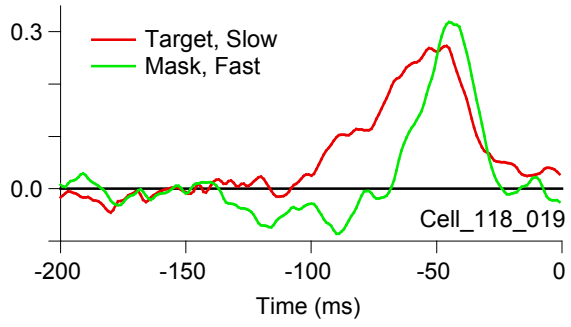
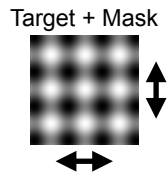
Recently, Higgs et al. [3] and Arsiero et al. [4] identified different forms of variance-dependent change in the  $f-I$  curves of



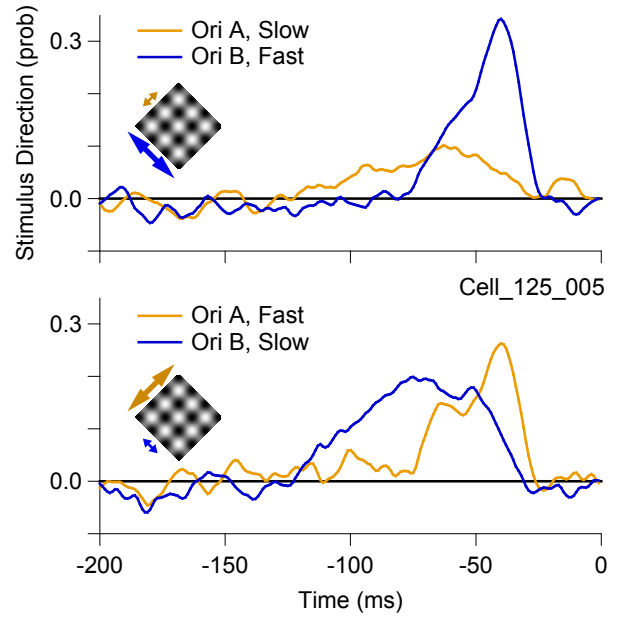
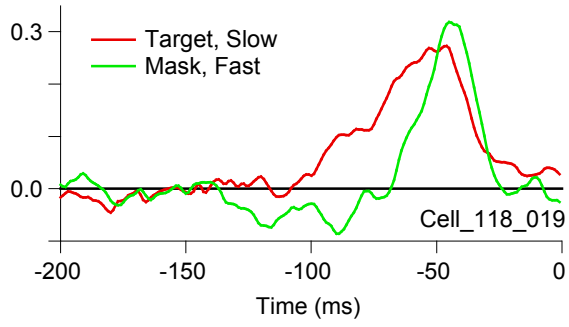
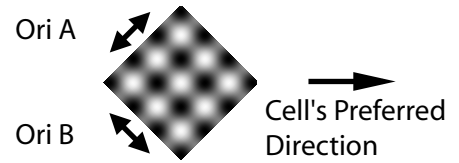
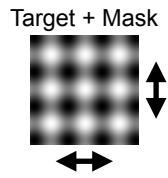
# Results for two V1 complex DS cells



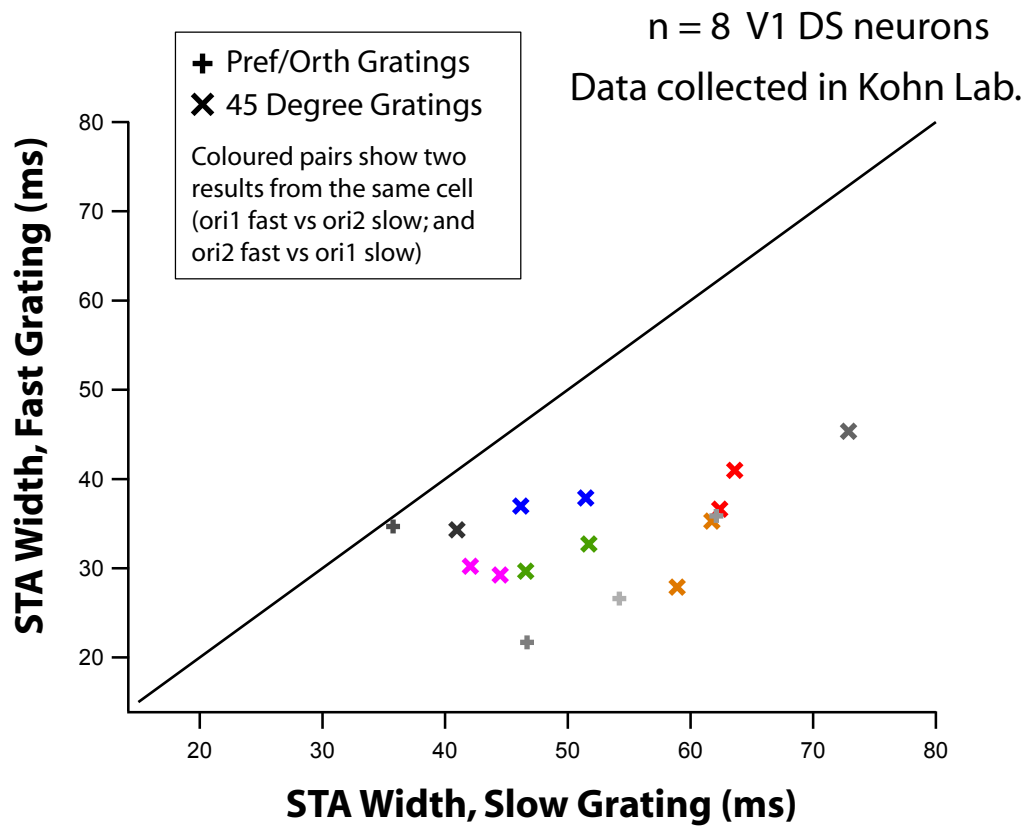
# Comparing Target and Mask STAs



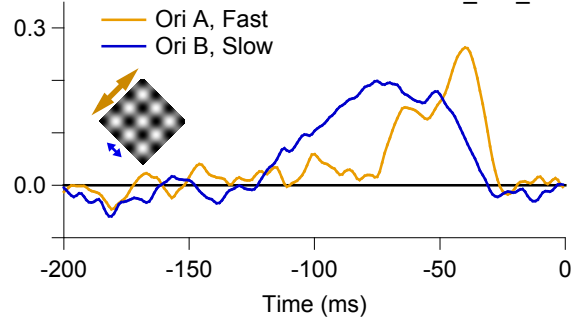
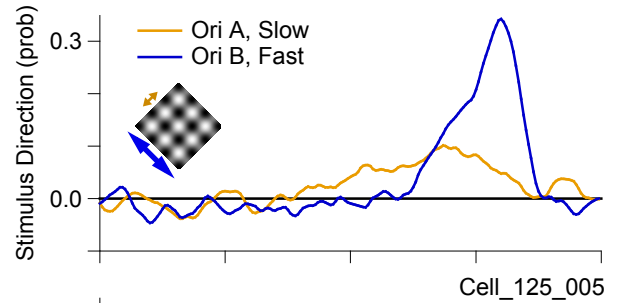
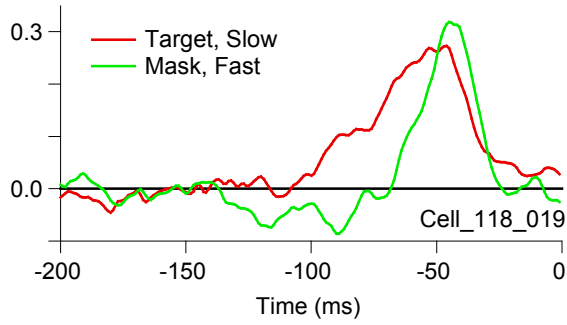
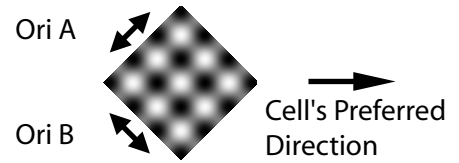
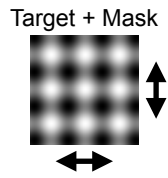
# Comparing Target and Mask STAs



# Comparison of STA width for Fast vs. Slow Components

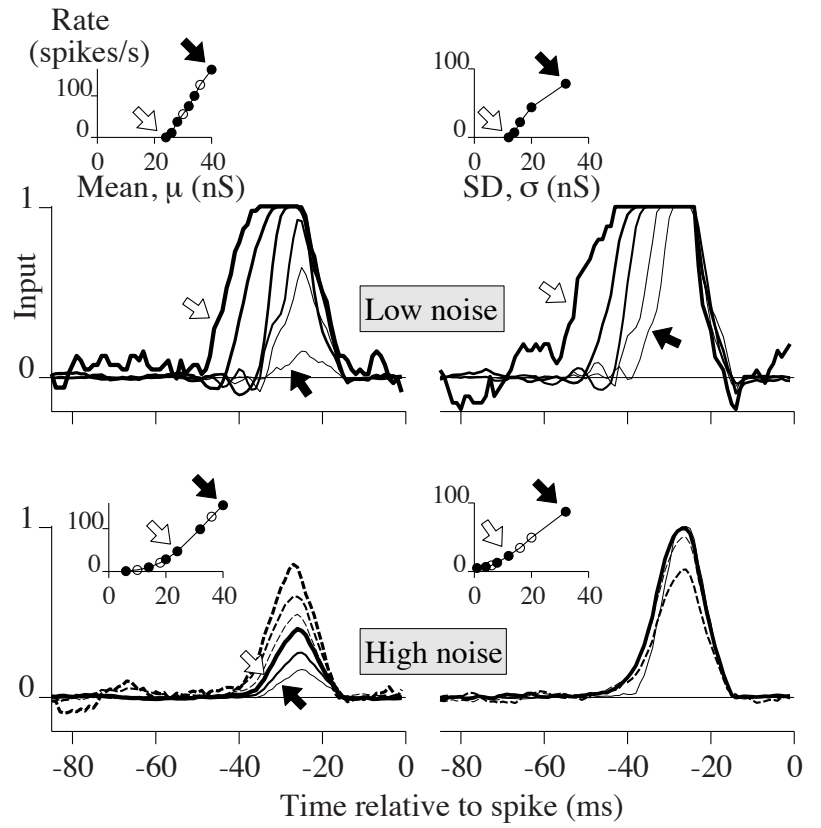
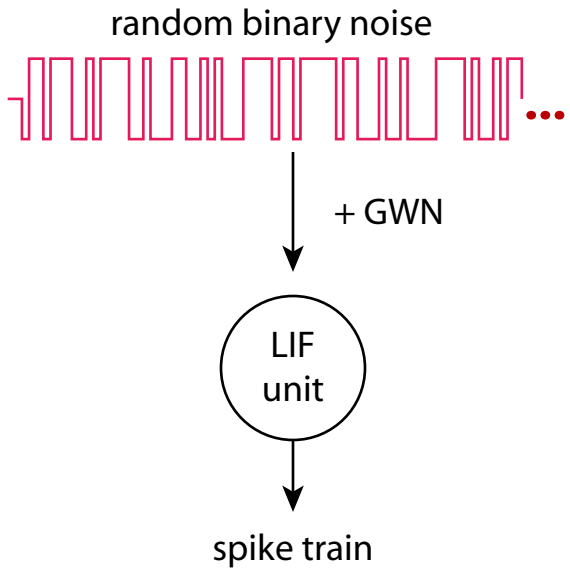


# Comparing Target and Mask STAs



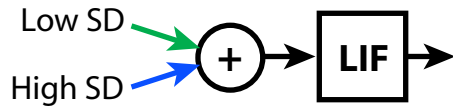
**Multitemporal encoding**

# Noisy input to leaky integrate-and-fire unit

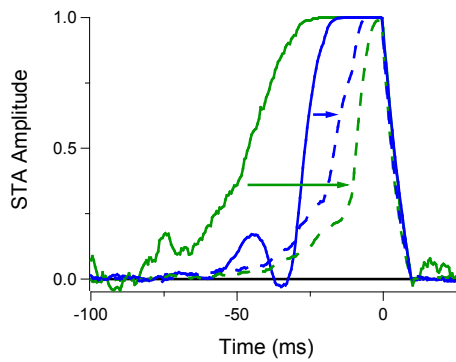


# Multitemporal Encoding in Models

**Linear integrate and fire, with binary, white noise inputs**

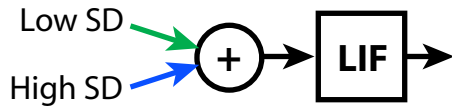


- Low SD isolated
- - Low SD combined
- High SD isolated
- - High SD combined

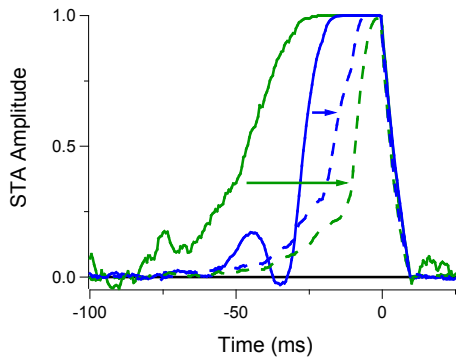


# Multitemporal Encoding in Models

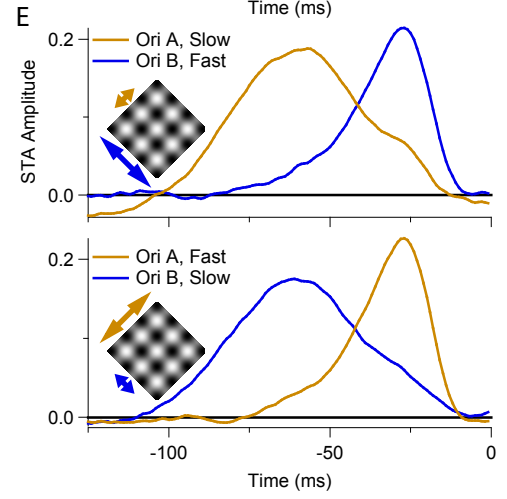
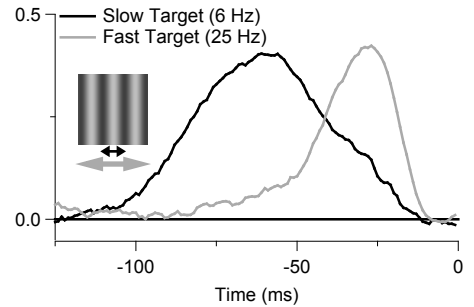
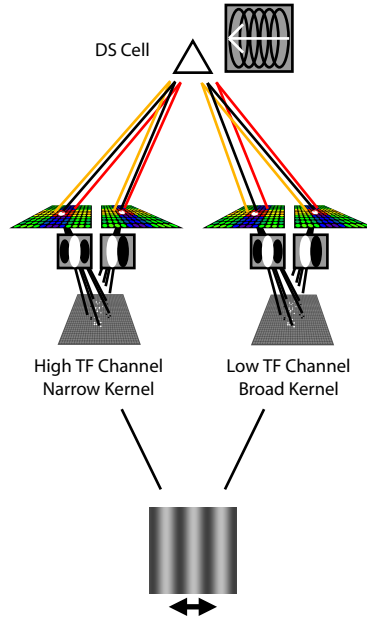
**Linear integrate and fire, with binary, white noise inputs**



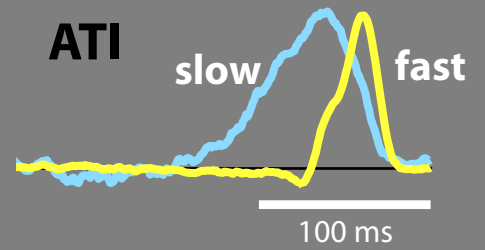
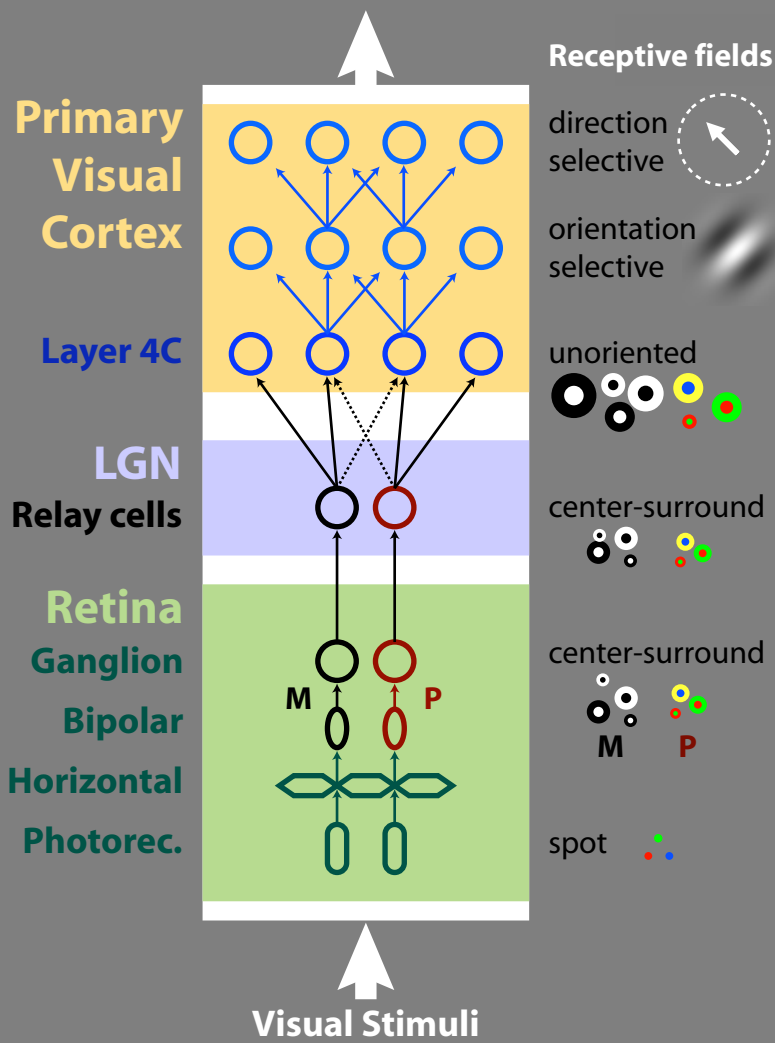
- Low SD isolated
- - Low SD combined
- High SD isolated
- - High SD combined



**Spiking network of conductance-driven leaky I & F neurons**



# Visual motion pathway, retina to V1



## How could ATI arise?

- X-** Changes in the retina
- X-** Cortical normalization
- X-** Adaptation at the soma
- X-** Non-linear interaction at spike generation
- Parallel pathways: convergence of fast and slow channels

**ATI is channel specific.**  
**Multitemporal encoding in DS neurons.**

# Temporal integration in visual cortex

## Summary

Channel-specific control of temporal integration

No evidence for cortical normalization

Multitemporal encoding - the multiplexing of distinct temporal signals, reflected in the spike discharge of a single neuron

A parallel pathway model can account for the data.

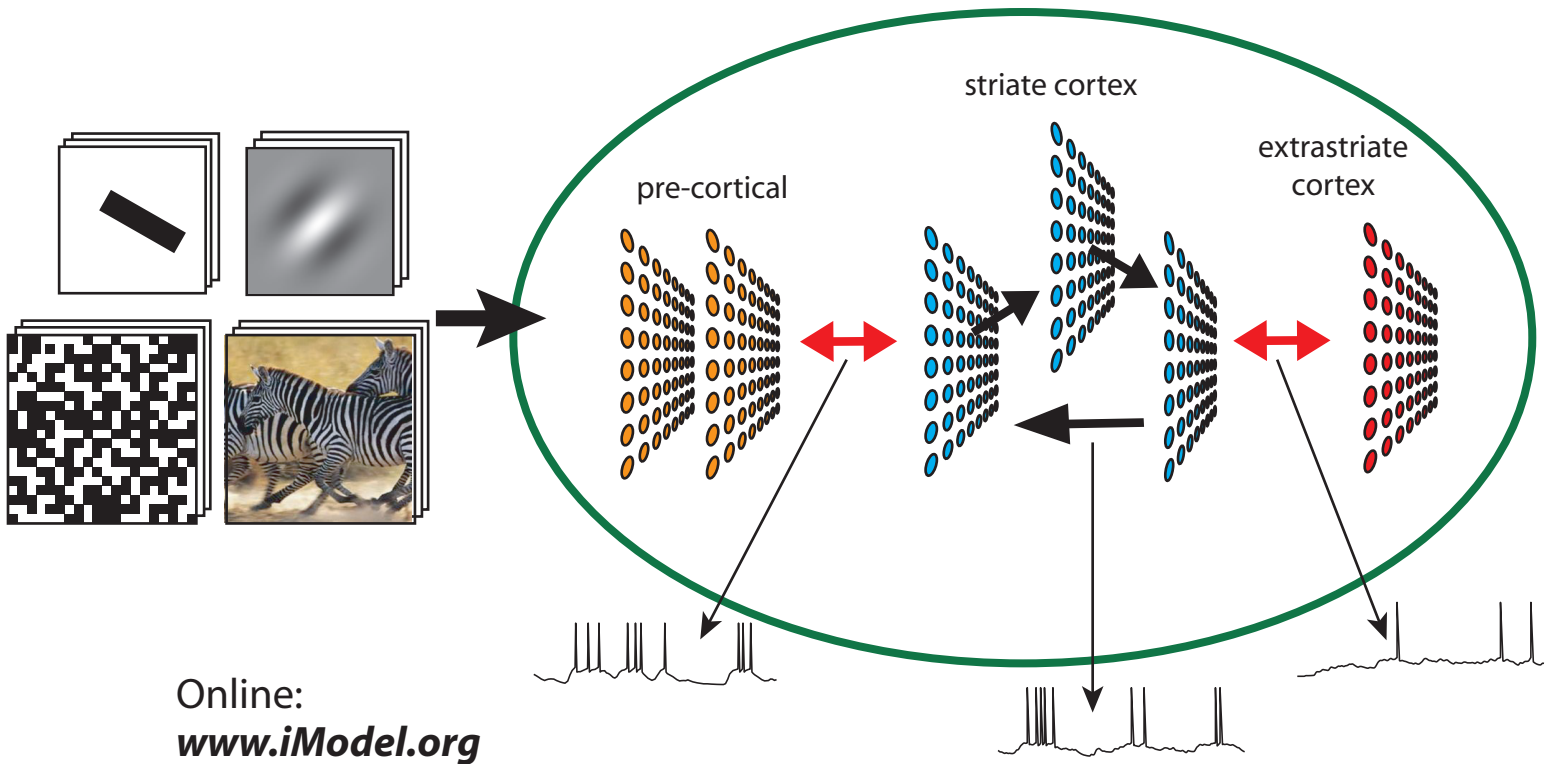
# A principled approach to modelling

**Modularity** - local representation of computation

**Emulation** - responses resemble those recorded in major cell classes

**Applicability** - accept arbitrary, time-varying stimuli

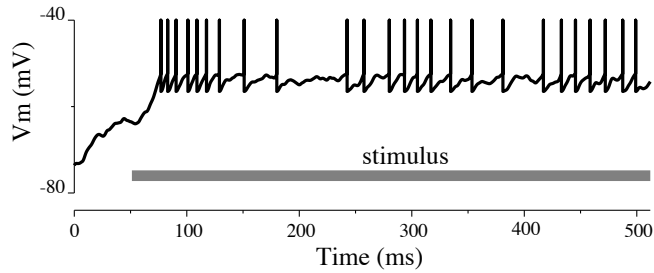
**Accessibility** - available on the web, fast computation is cheap



# Spiking Units

## Conductance-driven leaky integrate-and-fire (LIF) units

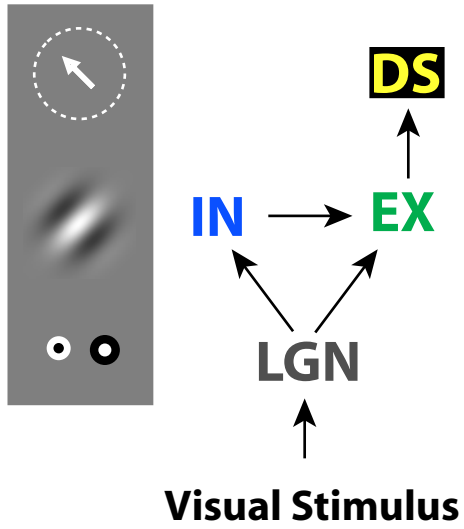
$$C \frac{dV}{dt} = g_{\text{ex}}(V_{\text{ex}} - V) + g_{\text{in}}(V_{\text{in}} - V) + g_{\text{leak}}(V_{\text{rest}} - V)$$



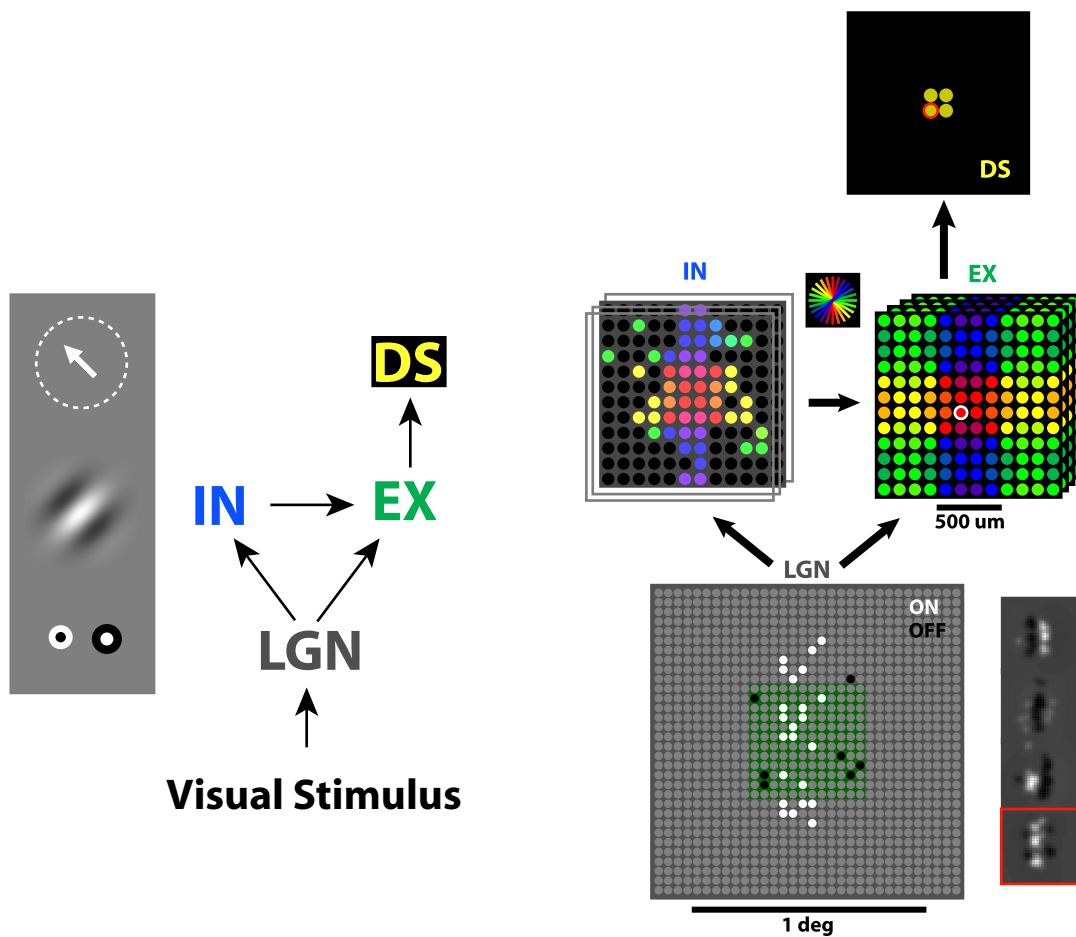
**Noise is added to  $g$ 's**

**Non-linear interactions between "dendritic" inputs**

# A circuit implementation for building V1 DS neurons



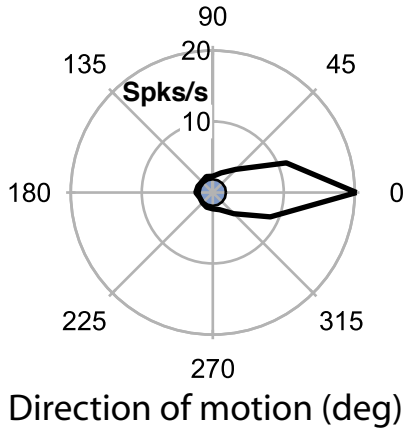
# A circuit implementation for building V1 DS neurons



- Populations of conductance-driven spiking units
- Physiological RF attributes: ON/OFF, orientation, spatial frequency & phase
- Physiologically realistic synaptic time course
- Driven by a wide variety of visual stimuli

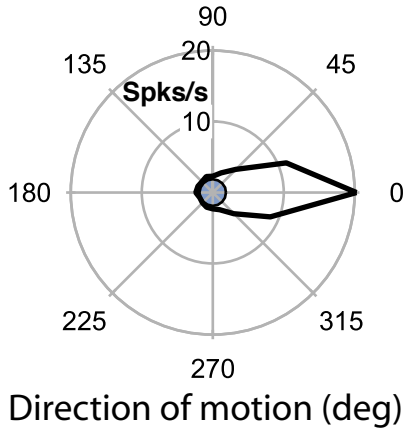
# Creating Direction Selectivity

## Direction tuning curve



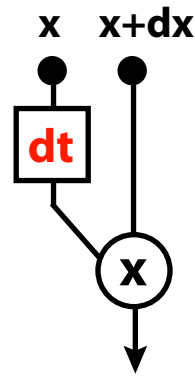
# Creating Direction Selectivity

## Direction tuning curve



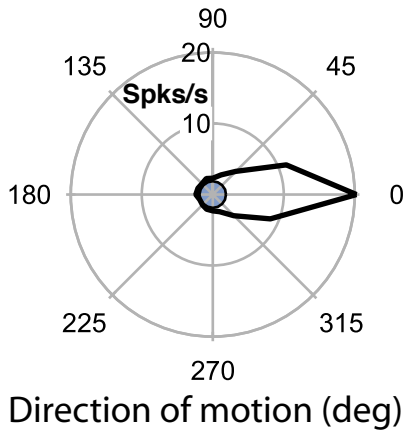
## Reichardt mechanism

Reichardt (1957)



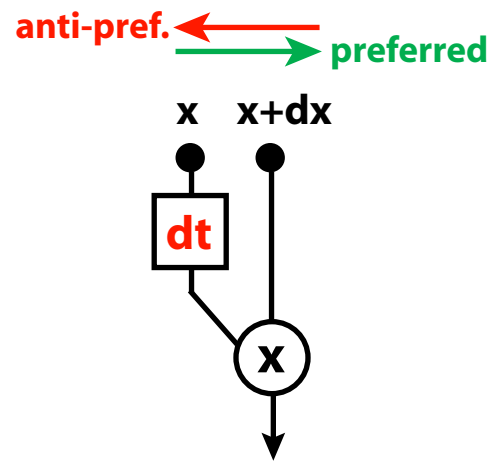
# Creating Direction Selectivity

## Direction tuning curve



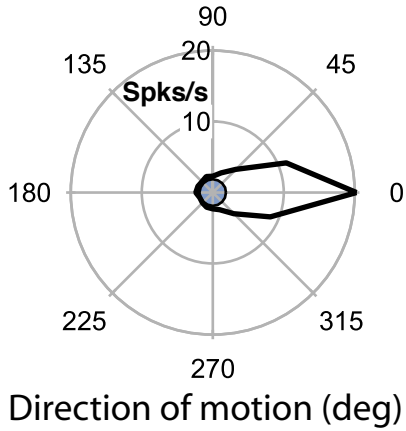
## Reichardt mechanism

Reichardt (1957)



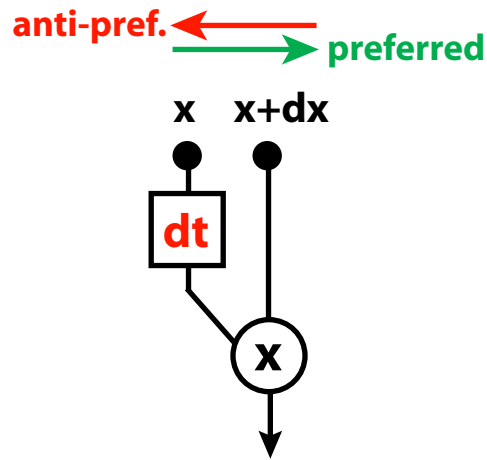
# Creating Direction Selectivity

## Direction tuning curve



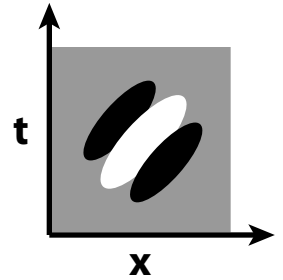
## Reichardt mechanism

Reichardt (1957)



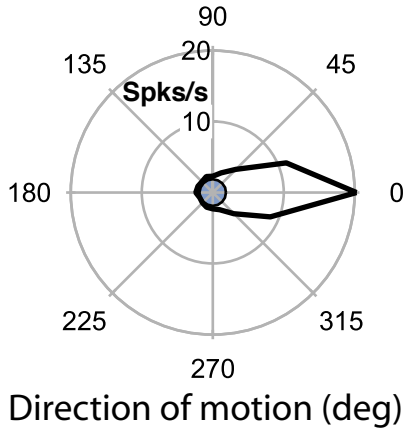
## Tilted X-T filter

Adelson & Bergen (1985)



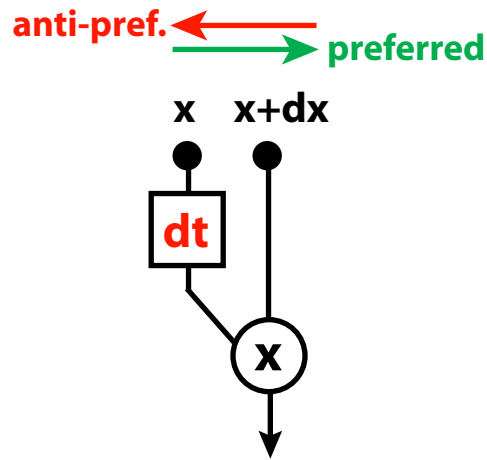
# Creating Direction Selectivity

## Direction tuning curve



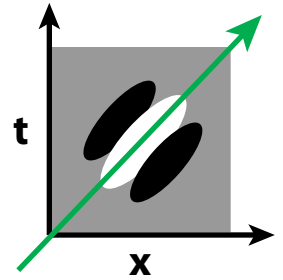
## Reichardt mechanism

Reichardt (1957)



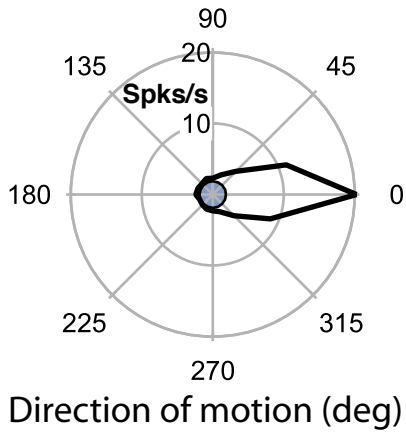
## Tilted X-T filter

Adelson & Bergen (1985)



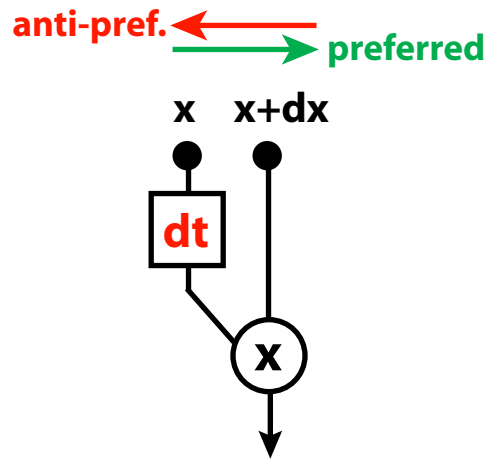
# Creating Direction Selectivity

## Direction tuning curve



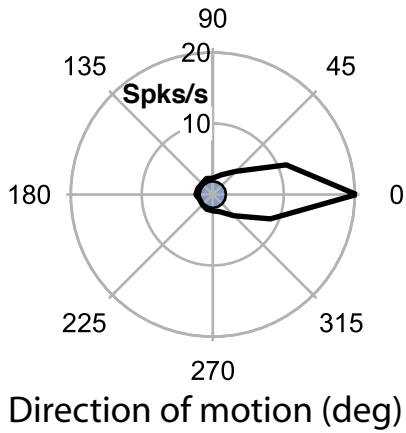
## Reichardt mechanism

Reichardt (1957)



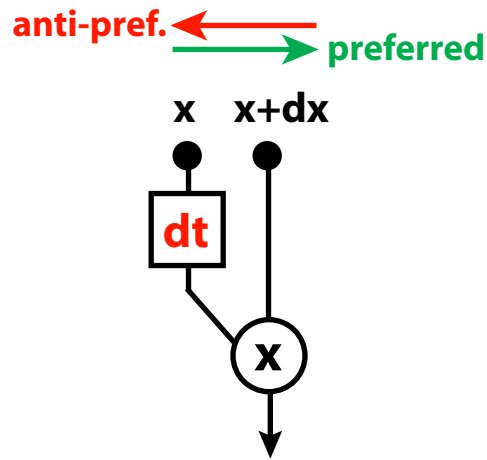
# Creating Direction Selectivity

## Direction tuning curve

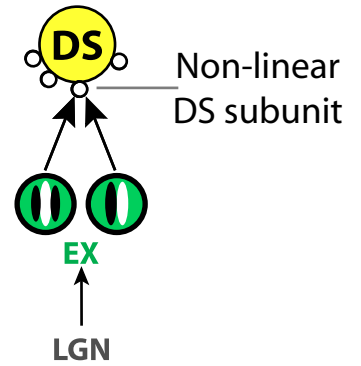


## Reichardt mechanism

Reichardt (1957)

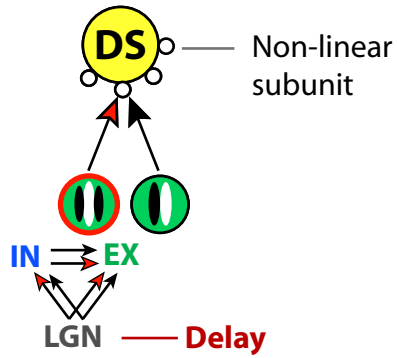


## Network implementation



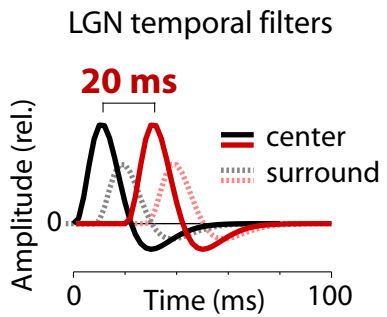
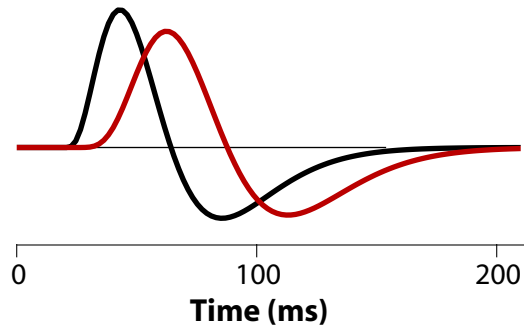
Torre and Poggio, 1978  
Koch, Poggio & Torre, 1983  
Polisky et al., 2004

# Presynaptic Delay: Delay in Inputs



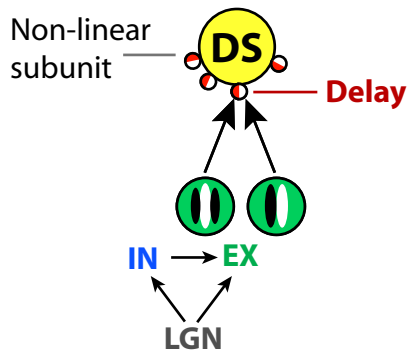
## Temporal diversity in V1 and LGN

Adelson and Bergen (1985)  
De Valois and Cottaris (1998)

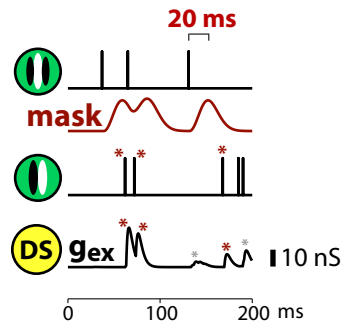


## Single-filter DS model

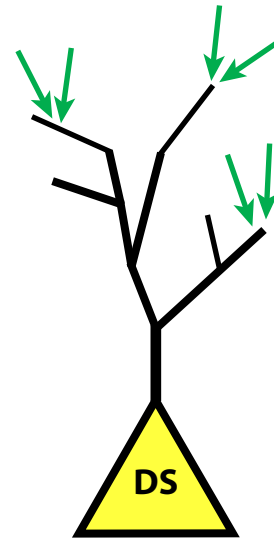
# Postsynaptic Delay: Delay in Dendrites



## Subunit interaction

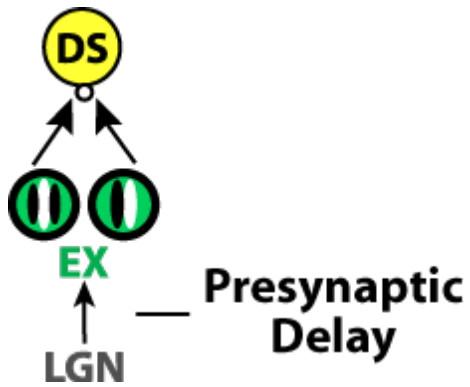
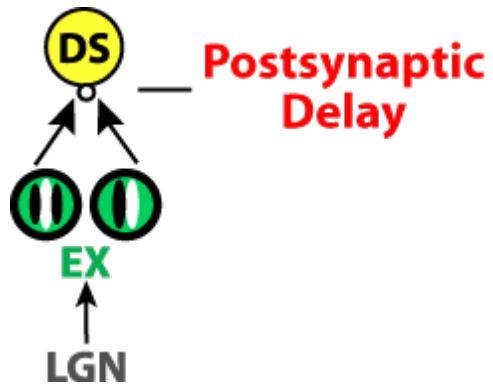


## Dendritic subunits

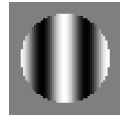


Torre and Poggio, 1978  
Branco et al., 2010

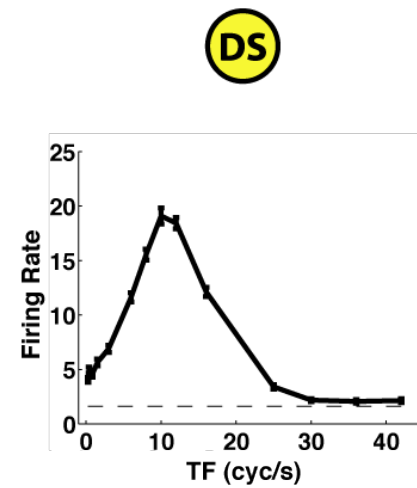
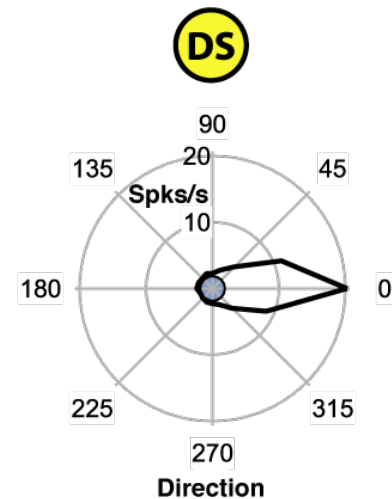
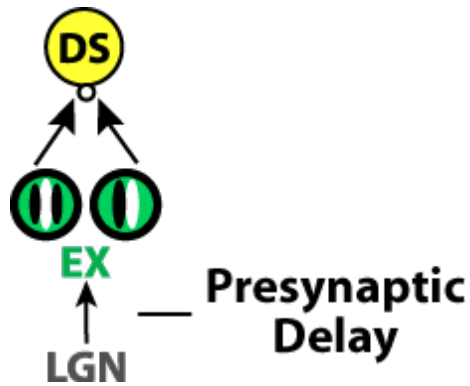
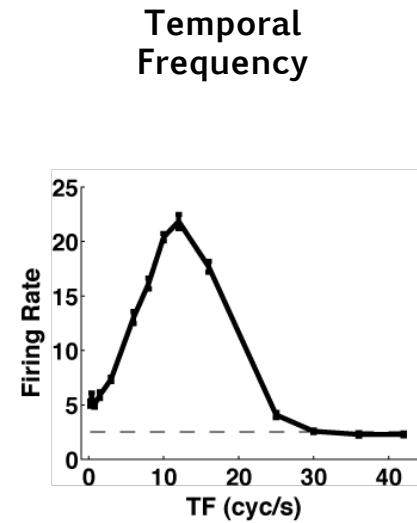
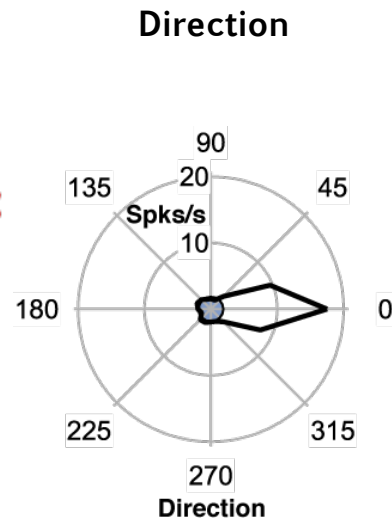
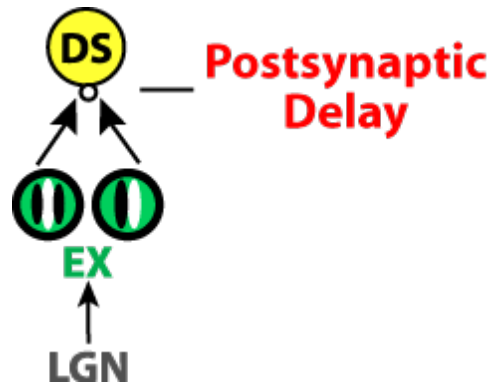
# Comparing models with pre- and postsynaptic DS delays



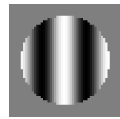
# Comparing models with pre- and postsynaptic DS delays



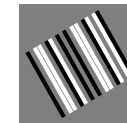
Drifting Gratings



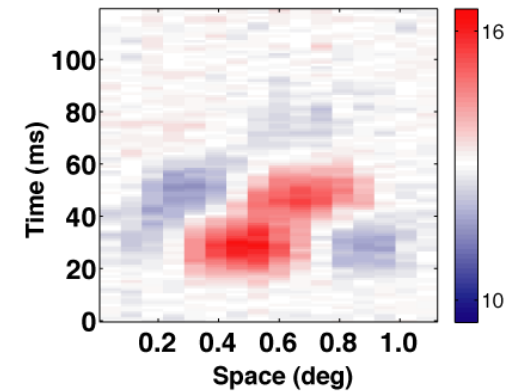
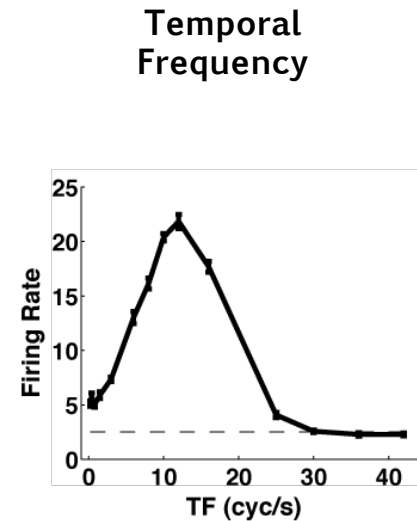
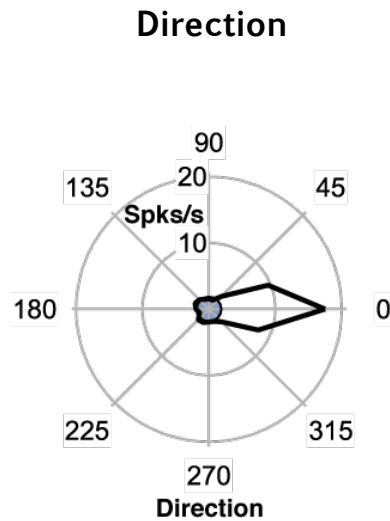
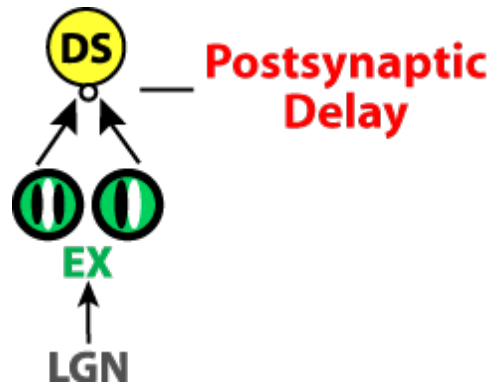
# Comparing models with pre- and postsynaptic DS delays



Drifting Gratings



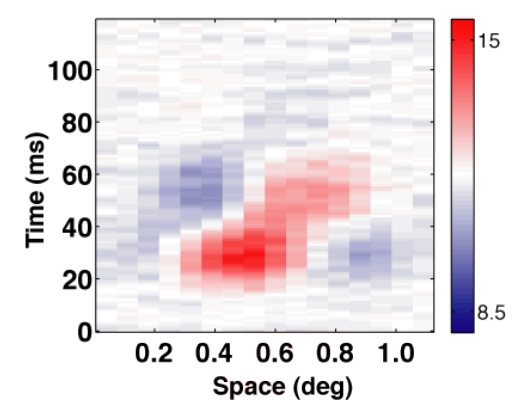
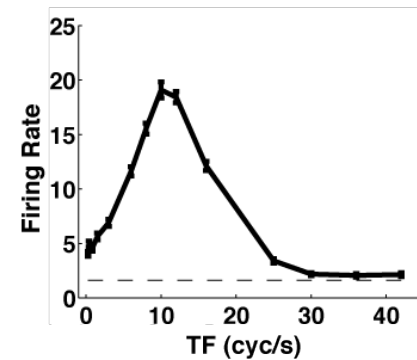
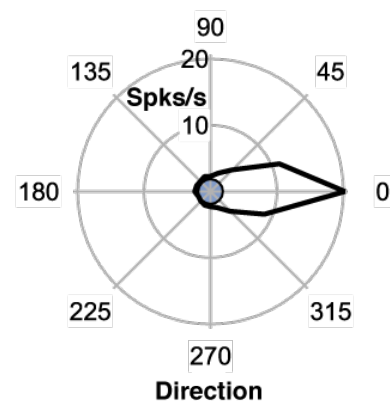
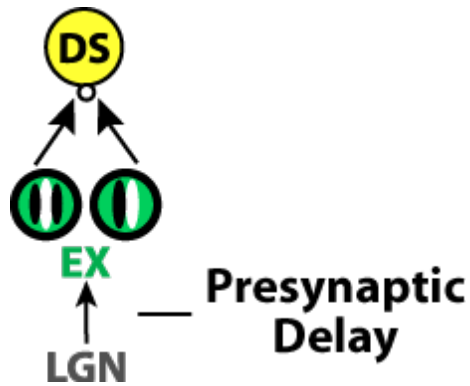
1D White Noise



DS

DS

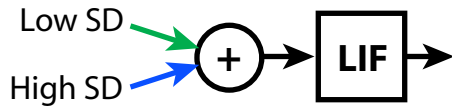
DS



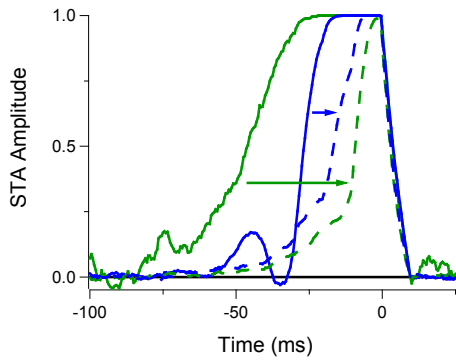
# Model Demo

# Multitemporal Encoding in Models

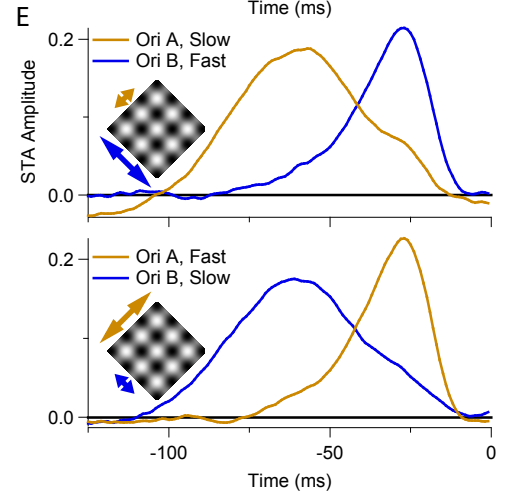
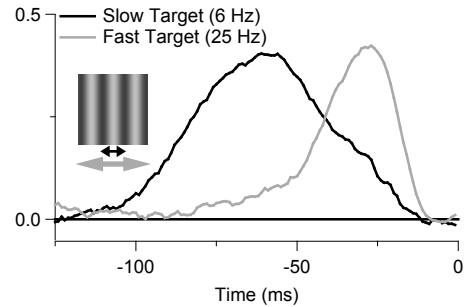
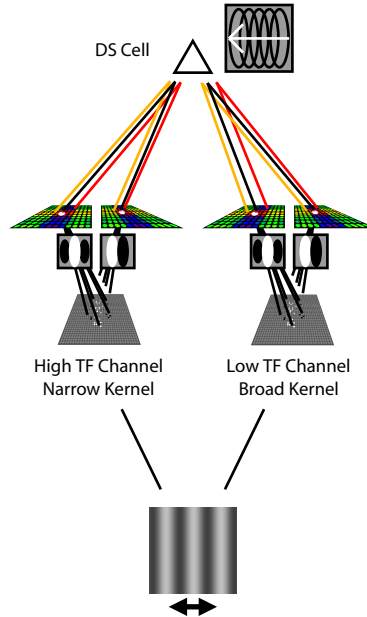
**Linear integrate and fire, with binary, white noise inputs**



- Low SD isolated
- - Low SD combined
- High SD isolated
- - High SD combined



**Spiking network of conductance-driven leaky I & F neurons**



## Related models

[DS\\_Post\\_Fac](#)  
[DS\\_Post\\_Sup](#)  
[DS\\_Pre\\_Fac](#)  
[DS\\_Pre\\_Sup](#)

## Variations

[DS\\_Post\\_Fac](#)

## DS\_Post\_Fac

## Direction Selective, Post-Synaptic, Facilitatory

## Summary

Complex direction selective (DS) cells are created within a spiking network model from pair-wise interactions of spiking inputs from non-DS, orientation-tuned simple cells. The DS interaction involves (i) cell pairs with spatial RFs that are phase-offset by about 90 deg, (ii) a temporal delay that is implemented **post-synaptically** (relative to the synapse at the transformation from non-DS to DS), and (iii) a **facilitatory** interaction. This is a hierarchical model containing four distinct populations of spiking units: LGN (ON and OFF center), V1 simple inhibitory, simple excitatory, and complex DS. The spiking cells are conductance-driven integrate and fire units modeled on those of Troyer et al. (1998).

[View Model](#)

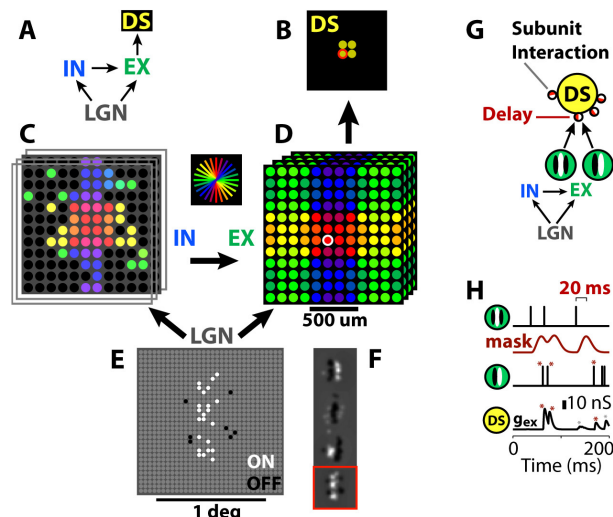
DS\_Post\_Fac

## Results

To be added. Under development. Apr 2010.

## References

- Baker PM, Bair W (2010) Cross-correlation analysis reveals circuits and mechanisms underlying direction selectivity. Conference Abstract: Computational and Systems Neuroscience 2010. doi: 10.3389/conf.fnins.2010.03.00332



www.iModel.org

DS\_Post\_Fac

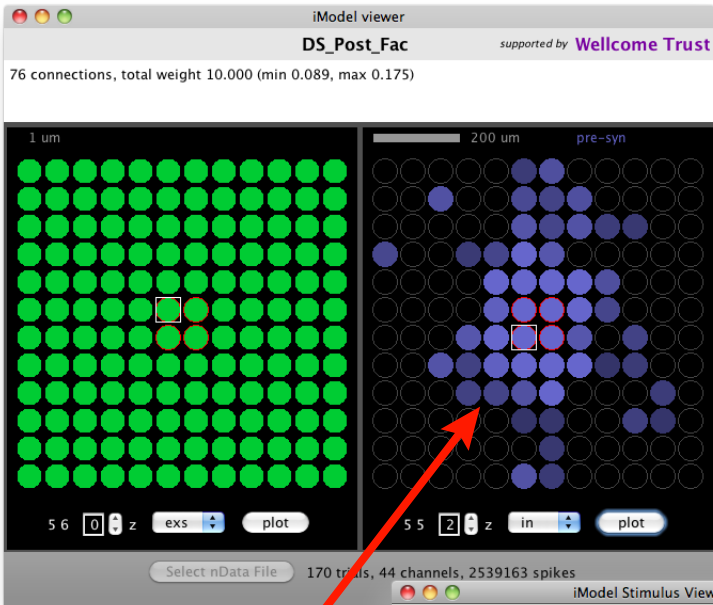
(A) Organization of the four populations of spiking units: LGN-lateral geniculate nucleus, IN-inhibitory V1 simple cells, EX-excitatory V1 simple cells, DS-direction selective V1 cells.

(B) A population of four V1 DS complex cells.

(C) Within a 12,12,4 (x,y,z) lattice of V1 inhibitory simple cells (IN), cells in the 3rd z-layer that are presynaptic to the white-circled cell in (D) are shown in color. Colors indicate preferred orientation (see orientation key between panels C and D).

(D) The 12,12,4 lattice of V1 excitatory simple cells (EX) is shown where color indicates orientation (see orientation key). The white-circled cell gets IN inputs as marked in (C) and

# Model Viewer



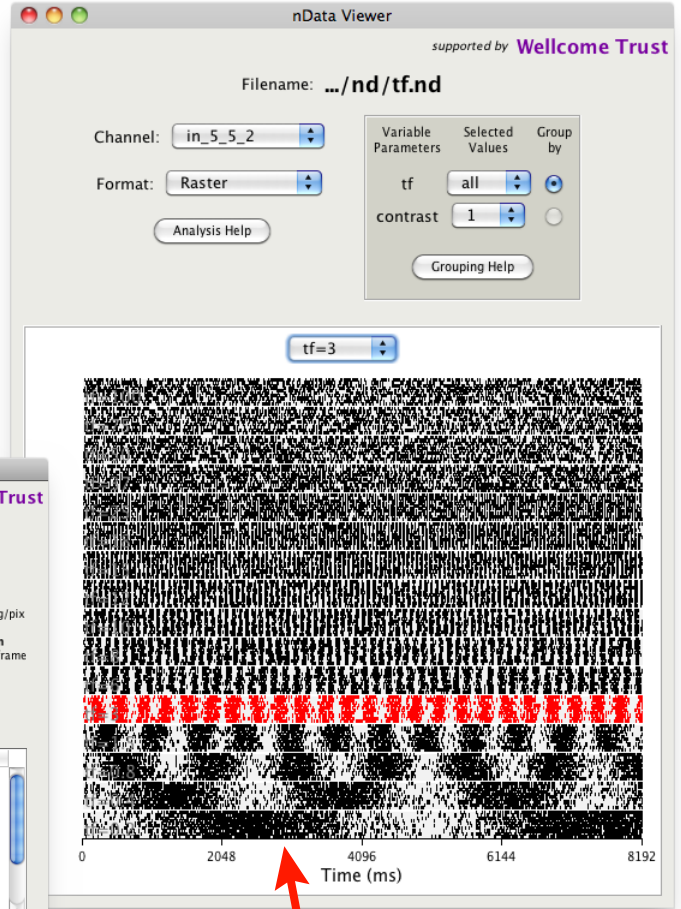
Synaptic weight patterns

# Stimulus Editor/Player



# iModel Tools

# Response Viewer / Analyzer



Neuronal responses: action potentials

# Summary

**We developed a set of spiking network models for DS circuits motivated by several popular theories.**

**The models offer insight for developing experimental solutions to some of the fundamental questions about DS neurons.**

**We are developing interactive tools to make it easy for others to explore and test the models.**

# Acknowledgements

**University of Oxford**

**Douglas McLelland**

**Pamela Baker**

**Bashir Ahmed**

**Also thanks to:**

**Adam Kohn**



**welcome**trust



**St John's College**  
Oxford